Journal of Sedimentary Research

Journal of Sedimentary Research, 2008, v. 78, 199–219
Research Article
DOI: 10.2110/jsr.2008.022

RE-EVALUATION OF THE MIDDLE MIOCENE EAGLE MOUNTAIN FORMATION AND ITS SIGNIFICANCE AS A PIERCING POINT FOR THE INTERPRETATION OF EXTREME EXTENSION ACROSS THE DEATH VALLEY REGION, CALIFORNIA, U.S.A.

BYRDIE RENIK,[1] NICHOLAS CHRISTIE-BLICK,[1] BENNIE W. TROXEL,[2] LAUREN A. WRIGHT,[3] AND NATHAN A. NIEMI[4]
[1]*Department of Earth and Environmental Sciences and Lamont-Doherty Earth Observatory of Columbia University, Palisades, New York 10964-8000, U.S.A.*
[2]*2961 Redwood Road, Napa, California 94558, U.S.A.*
[3]*Department of Geosciences, The Pennsylvania State University, University Park, Pennsylvania 16802, U.S.A.*
[4]*Department of Geological Sciences, 1100 North University Avenue, University of Michigan, Ann Arbor, Michigan 48109-1005, U.S.A.*
e-mail: renik@ldeo.columbia.edu

ABSTRACT: **The Death Valley area of eastern California and southern Nevada has been highly influential in the development of ideas about extreme crustal extension. One of the tightest constraints on Death Valley extension is apparently provided by clasts in inferred alluvial-fan deposits of the Eagle Mountain Formation (~ 15–11 Ma) and their source in the Hunter Mountain batholith, now located > 100 km from some of the deposits. Because alluvial fans are usually less than 10–20 km in radius, the remaining separation has been interpreted as tectonic. New research reported here suggests that the Eagle Mountain Formation at its type location was deposited in a fluvial–lacustrine setting, and provides no constraint on either the magnitude or the direction of tectonic transport and/or crustal extension. Confidence in palinspastic reconstruction thus depends on resolving ambiguities in the correlation of pre-extensional markers or on the recognition of demonstrably proximal facies tectonically distributed across the region.**

The succession at Eagle Mountain comprises (1) diffusely stratified monolithologic carbonate breccia and sandstone (~ 140 m) onlapping Cambrian carbonate rocks at an unconformity with ~ 110–140 m of relief (fluvial or fluvially influenced); (2) ~ 10 m of tabular-bedded siltstone, diamictite, and sandstone (lacustrine); (3) cross-stratified and channelized sandstone and polymict conglomerate bearing Hunter Mountain clasts, with minor siltstone and carbonate (~ 110 m; mostly fluvial); and (4) tabular-bedded sandstone, siltstone, and minor carbonate (~ 140 m; mostly lacustrine). Eight prominent stratigraphic discontinuities mapped within the third interval are characterized by up to 15 m of local erosional relief, and by abrupt upward coarsening from siltstone or carbonate to conglomerate or sandstone. A fluvial interpretation for the same critical part of the succession is based upon the existence of the mapped surfaces; the ubiquitous development of channels, trough cross-stratification, and upward fining trends (particularly between the mapped surfaces); and the abundance of well rounded clasts in conglomerate. Paleocurrents are generally directed between southward and eastward, although with considerable dispersion, and they shift from approximately southward or southeastward in the mostly fluvial deposits to approximately eastward in the upper lacustrine interval. An unusual feature of the Eagle Mountain Formation at Eagle Mountain is the presence of five crosscutting conglomerate bodies, interpreted as vertically infilled fissures of tectonic origin. Numerous normal, reversed normal, and oblique-slip faults with up to 34 m of stratigraphic separation are thought to postdate sedimentation and tilting of the Eagle Mountain Formation after ~ 11 Ma.

INTRODUCTION

The central Basin and Range Province of eastern California and southern Nevada, U.S.A., has proven influential in the development of ideas about mechanisms of crustal extension, quantified in that region through palinspastic reconstruction (Snow and Wernicke 2000; McQuarrie and Wernicke 2005). The premise of the palinspastic approach is that pre-extensional features such as isopachs, facies boundaries, thrust faults, folds, and paleoisothermal surfaces can be correlated and realigned to reveal the overall strain field. Such data have been assembled into what appears to be a particularly well constrained reconstruction across the Death Valley region of eastern California (Fig. 1; e.g., Snow and Wernicke 1989, 2000), purportedly one of the most highly extended parts of the Basin and Range (Snow and Wernicke 2000; Niemi et al. 2001; McQuarrie and Wernicke 2005). Nonetheless, uncertainties remain in structural correlation, in the depiction of isopachs and facies transitions, and in the pre-extensional configuration of all markers. This has left room for a considerable range of estimates for the amount of extension, from ~ 30–50% at the very least (Wright and Troxel 1973) to ~ 400–500% at the most (e.g., Stewart 1983; Wernicke et al. 1988a; Snow and Wernicke 2000; McQuarrie and Wernicke 2005). Specific correlations and alternative reconstructions have been the subject of vigorous debate

 1527-1404/08/078-199/$03.00

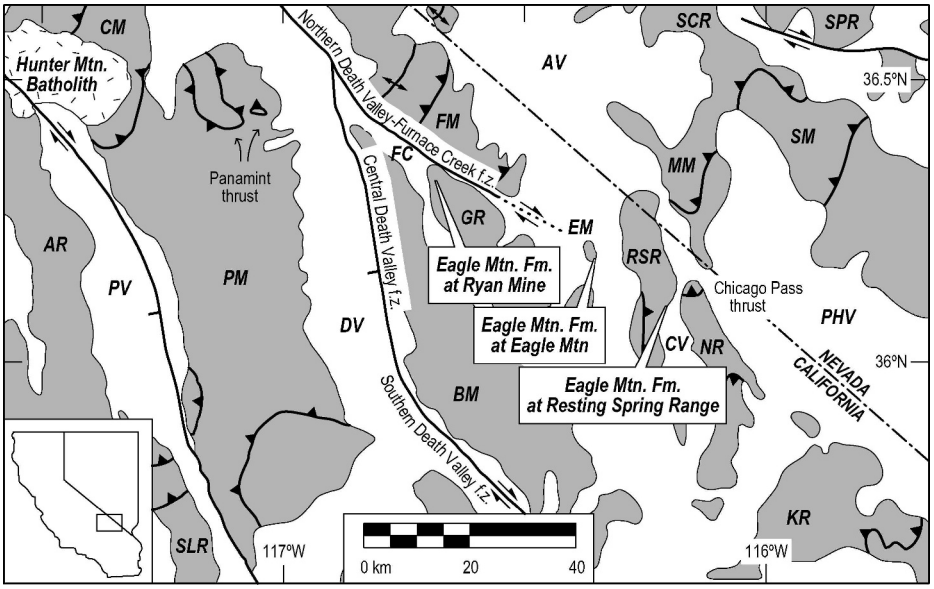

FIG. 1.—Physiographic map of Death Valley region showing locations of ranges (shaded) and valleys, selected late Paleozoic to Mesozoic contractile structures (teeth on upper plate of thrust faults), Cenozoic normal and strike-slip faults, distribution of Eagle Mountain Formation, and location of Hunter Mountain batholith (modified from Snow and Wernicke 2000; Niemi et al. 2001). Labeled thrust faults are those used to constrain specific palinspastic reconstructions in the area of interest (Wernicke et al. 1988a, 1988b; Snow and Wernicke 1989, 2000). Mountain range abbreviations: ***AR***–Argus Range, ***BM***–Black Mountains, ***CM***–Cottonwood Mountains, ***EM***–Eagle Mountain, ***FM***–Funeral Mountains, ***GR***–Greenwater Range, ***KR***–Kingston Range, ***MM***–Montgomery Mountains, ***NR***–Nopah Range, ***PM***–Panamint Mountains, ***RSR***–Resting Spring Range, ***SLR***–Slate Range, ***SCR***–Specter Range, ***SM***–Spring Mountains, ***SPR***–Spotted Range. Valley abbreviations: ***AV***–Amargosa Valley, ***CV***–Chicago Valley, ***DV***–Death Valley, ***FC***–Furnace Creek Wash, ***PHV***–Pahrump Valley, ***PV***–Panamint Valley. "Fault zone" is abbreviated ***f.z.***

(e.g., Stewart 1967, 1983, 1986; Wright and Troxel 1967, 1970; Stewart et al. 1968, 1970; Prave and Wright 1986a, 1986b; Corbett 1990; Wernicke et al. 1990; Stevens et al. 1991, 1992; Snow 1992a, 1992b; Snow and Wernicke 1993; Stone and Stevens 1993; Snow and Prave 1994; Serpa and Pavlis 1996; Çemen et al. 1999; Miller and Friedman 1999; Czajkowski and Miller 2001; Czajkowski 2002; Miller 2003; Çemen and Baucke 2005; Miller and Pavlis 2005; Stevens and Stone 2005, and references therein).

The middle Miocene Eagle Mountain Formation appears to provide a set of piercing points that circumvents the uncertainties and thus constitutes "some of the strongest direct evidence for major Tertiary displacements" (Snow and Wernicke 2000, p. 662). Inferred alluvial-fan conglomerate in this unit contains a distinctive clast assemblage that includes ~ 180 Ma leucomonzogabbro boulders (< 1 m) thought to have been derived from the Hunter Mountain batholith of the Cottonwood Mountains (CM in Figure 1), and to link the Eagle Mountain Formation with the compositionally comparable Entrance Narrows Member of the Navadu Formation at that location (Wernicke 1993; Snow and Lux 1999; Brady et al. 2000; Niemi et al. 2001; Niemi 2002). Because the batholith is now located more than 100 km from some of the deposits, and because alluvial fans are usually less than 10–20 km in radius, Niemi et al. (2001) concluded that tectonic transport was responsible for the separation of clasts and source beyond that distance. The present paper tests the hypothesis that the Hunter Mountain clasts were deposited by rivers rather than at alluvial fans—an idea first suggested but not developed by Çemen (1999) and by Wright et al. (1999). Most of our data come from the type locality of the Eagle Mountain Formation at Eagle Mountain, California (EM in Figure 1; Figs. 2, 3). Thirteen measured stratigraphic sections were correlated by tracing physical surfaces on a photographic panorama (~ 1 : 450 scale) and on stereopairs of color aerial photographs (1 : 740 scale) obtained under contract with Aero Tech Mapping (Figs. 3–5). We also used a Laser Technologies, Inc., Impulse 200 range finder with a MapStar digital compass to quantify the geometry and orientation of erosional relief. Exposures of the Eagle Mountain Formation at the Ryan mine in Furnace Creek Wash and in the Chicago Valley on the east side of the Resting Spring Range (FC, CV, and RSR in Figure 1) were visited for

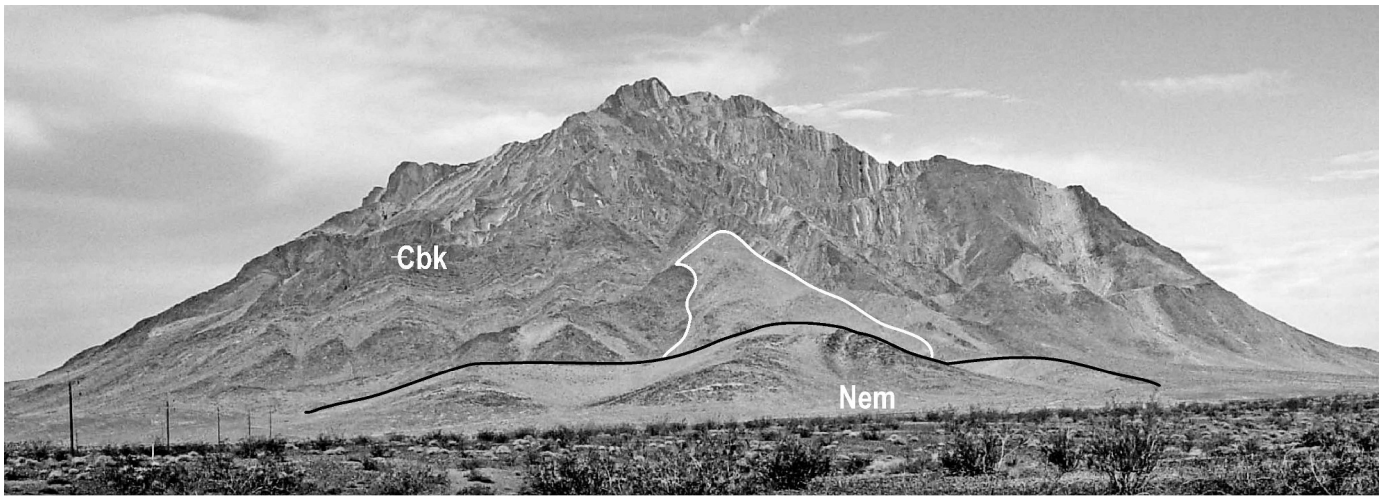

FIG. 2.—Eagle Mountain viewed from the southeast. Black line traces hill photographed in Figure 4 (where it is viewed from the opposite side). White line is trace of contact between Cambrian Bonanza King Formation (Ꞓbk) and middle Miocene Eagle Mountain Formation (Nem), which is hidden to the left by the hill.

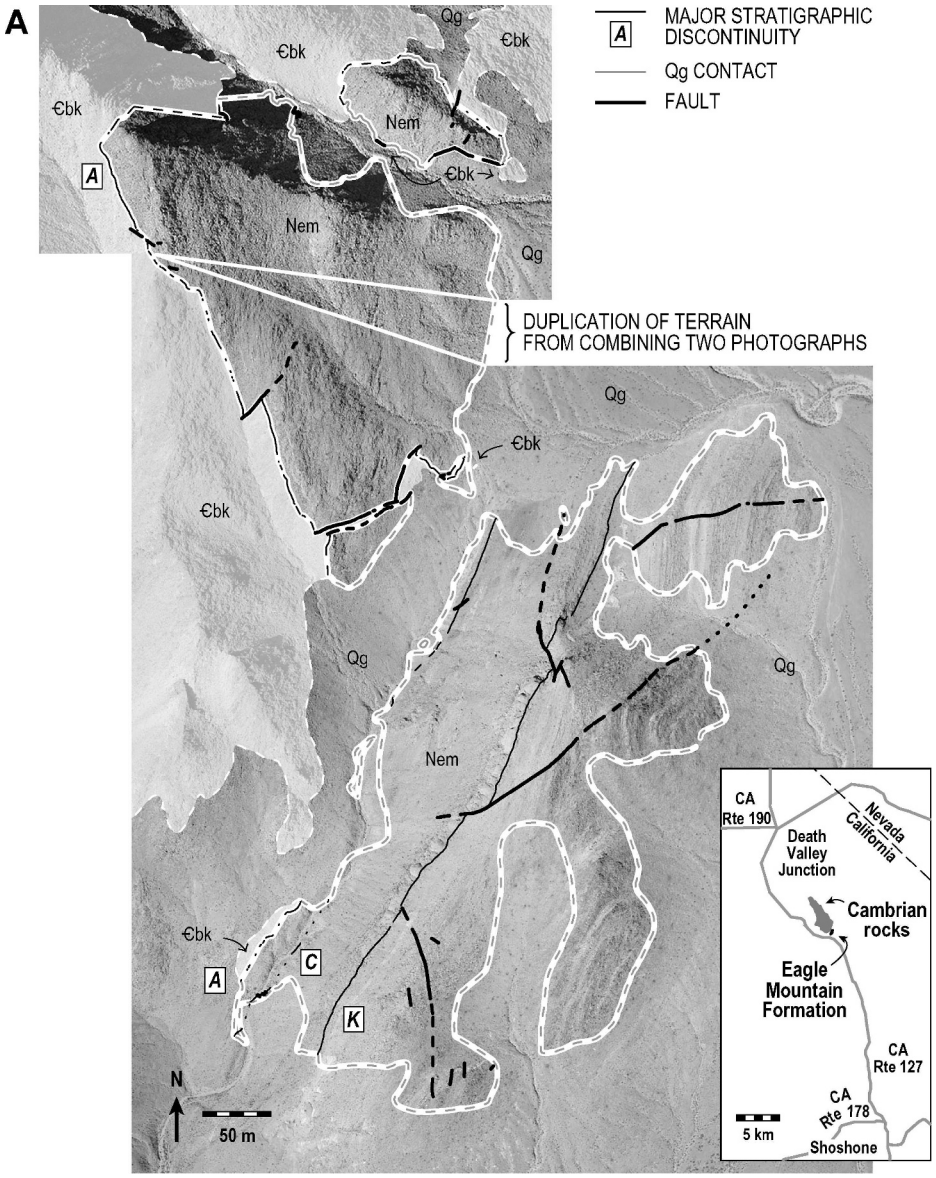

FIG. 3.—Maps of middle Miocene Eagle Mountain Formation at Eagle Mountain. **A)** Aerial photographs used as base for mapping and location of Eagle Mountain Formation at Eagle Mountain (inset). Versions of photographs used were in color and at a scale of 1:740. Stratigraphic contacts, major stratigraphic discontinuities (A, C, K), and faults are shown for reference, dashed where uncertain and dotted where concealed. Base of Miocene section and highest elevation is at northwest corner. Prominent ridge beneath (west of) surface K is conglomerate. Abbreviations: Cbk—Cambrian Bonanza King Formation (white overlay), Nem—Neogene Eagle Mountain Formation, Qg—Quaternary gravel. **B)** Geological map of Eagle Mountain Formation, including stratigraphic discontinuities and other mapped markers, faults, crosscutting conglomerate bodies, and four intervals distinguished by facies assemblages, and measured sections. Much of the breccia–sandstone outcrop and the interval stratigraphically above surface L are dip slopes. Insets show details.

comparison. The Resting Spring Range outcrops, which are restricted to gullies and subject to structural complications, proved to be too limited to yield much independent information pertinent to the facies interpretation.

GEOLOGICAL SETTING

Cenozoic extension in the Death Valley region is only the most recent event in a protracted geological history. Crystalline basement rocks as old as 1.7 Ga are overlain discontinuously by the > 1.08 Ga to ~ 675 Ma Pahrump Group: up to ~ 3–4 km of clastic, carbonate, and minor volcanic rocks deposited at least partly in intracratonic rift basins (Burchfiel et al. 1992; Heaman and Grotzinger 1992; Wright and Prave 1993; Fanning and Link 2004). Upper Neoproterozoic to lower Paleozoic clastic and carbonate rocks form a westward-thickening wedge (< 11 km) representing minor renewed rifting and the development of a passive continental margin (Stewart 1972; Wright et al. 1981; Wernicke et al. 1988a; Wernicke et al. 1998b; Levy and Christie-Blick 1991; Link et al. 1993). A regional angular unconformity of Late Devonian age marks the onset of convergent margin tectonics (e.g., Wernicke et al. 1988a; Burchfiel et al. 1992). Crustal shortening and strike-slip tectonics continued intermittently in the Death Valley region from the Permian to the Cretaceous, and are expressed today by thrust faults, folds, and arc-related igneous rocks (e.g., Stevens and Stone 1988; Snow et al. 1991; Burchfiel et al. 1992; Snow 1992a). Coeval sedimentary rocks are present only locally within the orogen (Jennings et al. 1962; Streitz and Stinson 1974). Oligocene and younger sedimentary and volcanic deposits unconformably overlie rocks of Proterozoic to Permian age (Wright and Troxel 1984; Çemen et al. 1985; Çemen et al. 1999; Wernicke et al. 1988b; Holm and Wernicke 1990; Topping 1993; Çemen 1999; Snow and Lux 1999; Wright et al. 1999, and mapping referenced therein; Snow and Wernicke 2000; Niemi et al. 2001; Miller and Prave 2002; Miller and Pavlis 2005), at least in part as a result of exhumation, tilting, and dissection prior to the onset of Basin and Range extension (Miller and Pavlis 2005; cf. Stewart 1983).

Large-scale, northwest–southeast extension responsible for the contemporary block-faulted topography began during the Neogene (Wernicke et al. 1988a; Burchfiel et al. 1992; Wernicke 1992; Snow and Wernicke 2000). The palinspastic reconstruction described above suggests

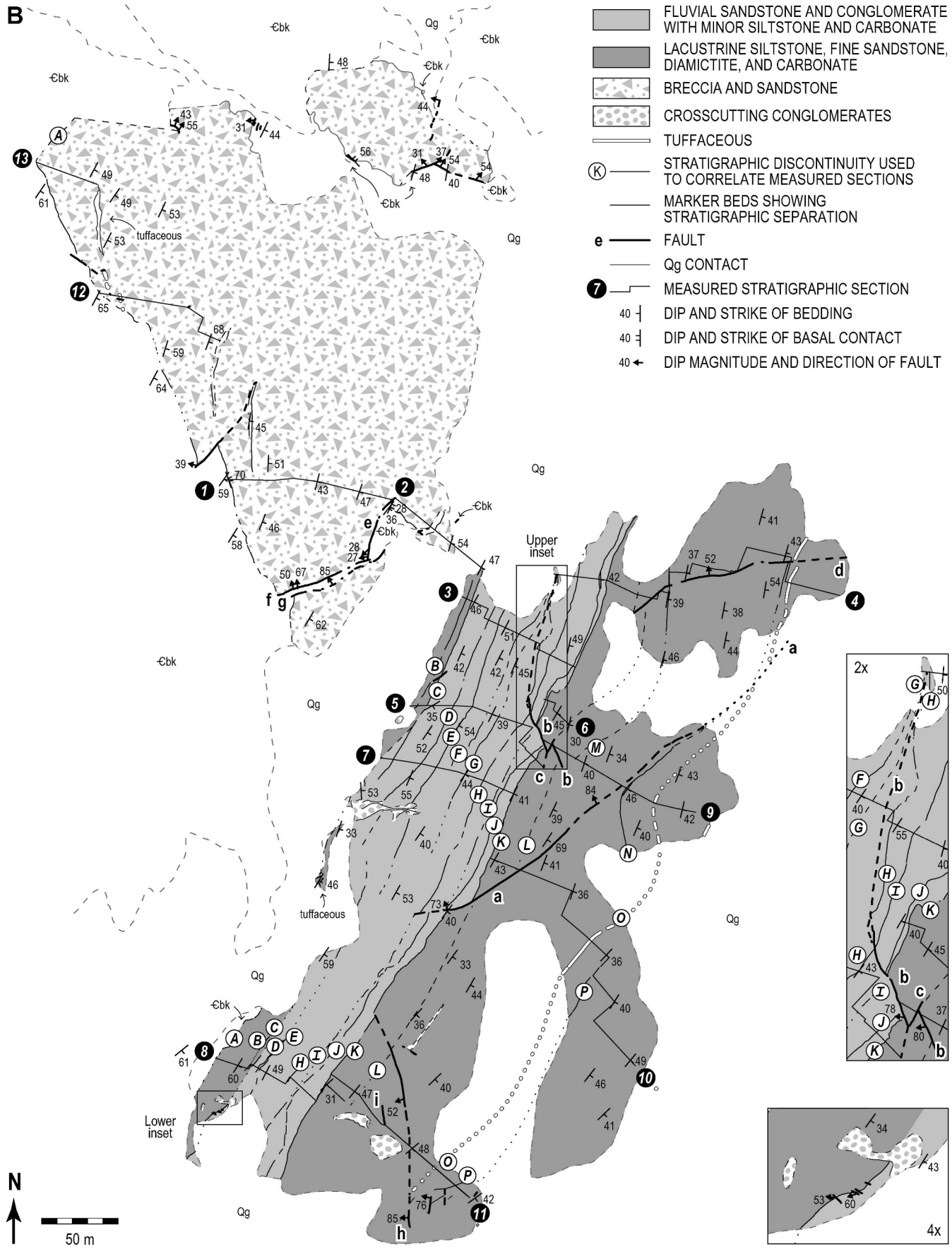

FIG. 3.—Continued.

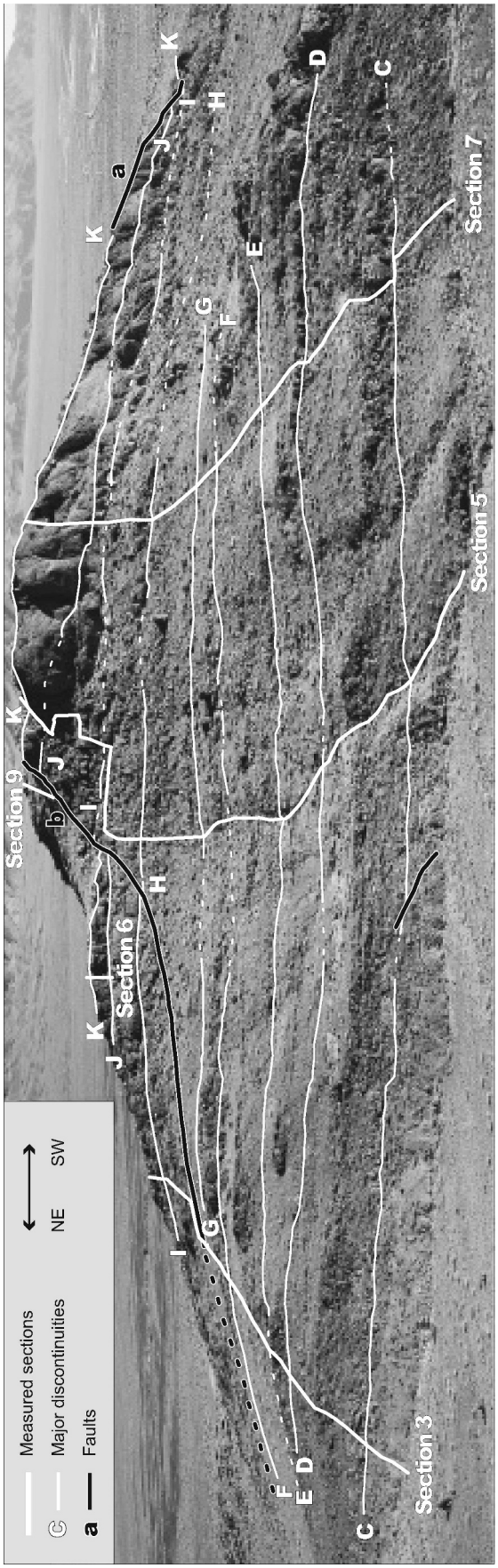

FIG. 4.—Middle fluvial–lacustrine interval of Eagle Mountain Formation, viewed from the northwest, showing parts of measured sections 3, 5, 6, 7, and 9, as well as mapped surfaces C–K and faults. Hunter Mountain clasts are found exclusively within this interval.

that extension was particularly great and is especially well constrained between the southern Cottonwood–northern Panamint Mountains and the Nopah Range (CM, PM, and NR in Figure 1). Structural restoration in that area is based on diverse markers offset across the Northern Death Valley–Furnace Creek fault zone (Fig. 1; McKee 1968; Stewart 1983; Snow and Wernicke 1989, 2000) and on correlation of the Panamint and Chicago Pass thrust faults (Wernicke et al. 1988a; Wernicke et al. 1988b; Wernicke et al. 1988c; Niemi et al. 2001; cf. Serpa and Pavlis 1996; Miller and Pavlis 2005). Particular support for that correlation comes from the argument that the Hunter Mountain batholith (near the Panamint thrust fault) and the Eagle Mountain Formation (near the Chicago Pass thrust fault) were adjacent during middle Miocene time (Fig. 1; Çemen 1999; Brady et al. 2000; Niemi et al. 2001). The correlation of the thrust faults implies ~ 92 km of offset, and the latter match suggests ~ 104 km of total translation (Wernicke 1993; Niemi et al. 2001).

DESCRIPTION OF THE EAGLE MOUNTAIN FORMATION

The middle Miocene Eagle Mountain Formation (defined by Niemi et al. 2001) consists of as much as several hundred meters of sandstone, breccia, conglomerate, siltstone, carbonate, tephra, and diamictite (listed here from most to least abundant; Brady et al. 2000; Niemi et al. 2001). The rocks crop out discontinuously in the vicinity of Furnace Creek Wash, at Eagle Mountain, and in the Chicago Valley on the east flank of the Resting Spring Range (FC, EM, and CV in Figure 1). They unconformably overlie the Cambrian Zabriskie Quartzite, the Carrara Formation (with some uncertainty), and the Bonanza King Formation (Troxel 1989; Brady et al. 2000; Niemi et al. 2001). The age of the unit is best constrained by $^{40}Ar/^{39}Ar$ tephra dates of 15.0 Ma near the base of the section in the Resting Spring Range, as well as 13.4 and 11.6 Ma near the base and top of the section at Eagle Mountain (Brady et al. 2000; Niemi et al. 2001). K-Ar analysis of an apparently younger (less tilted) ash-flow tuff at Resting Spring Pass yielded an age of 9.6 Ma (Troxel and Heydari 1982; Heydari 1986; Wright et al. 1991; Brady et al. 2000; Niemi et al. 2001). In the sections that follow, we refer primarily to the Eagle Mountain locality, where the rocks are best exposed.

The Eagle Mountain Formation at Eagle Mountain is ~ 400 m thick and unconformably overlies carbonate rocks of the Cambrian Bonanza King Formation. It consists of the following succession, divisible into four distinct intervals (Fig. 5):

1. diffusely stratified monolithologic carbonate breccia and sandstone with rare carbonate and tephra, internally channelized in places (~ 140 m, Fig. 5A);
2. parallel- and wavy-laminated, tabular-bedded siltstone and structureless diamictite, with minor sandstone and rare tephra (~ 10 m, below surface C in Figure 5B; tephra shown in Figure 3B);
3. abundantly cross-stratified and channelized sandstone and polymict conglomerate, with minor siltstone and carbonate (~ 110 m, above surface C in Figure 5B); and
4. parallel- and wavy-laminated, tabular-bedded sandstone, siltstone, and minor carbonate and tephra, with sandstone most abundant at the top of the section (~ 140 m, Fig. 5C).

In the lowest three of these intervals (below surface K in Figure 5B), the Eagle Mountain Formation thickens to the north-northeast, from ~ 75 m at section 8 to ~ 250 m at sections 13, 12, and 1–3 (Figs. 3B, 5). This is accomplished primarily by onlap against the basal contact and by more general thickening in the third interval (Figs. 3B, 5). No comparable thickening can be documented at other stratigraphic levels, although details of the uppermost 140 m above surface K are obscured by the presence of faults and incomplete outcrop.

A set of 180 tilt-corrected paleocurrent measurements indicates flow generally between southward and eastward, although with considerable

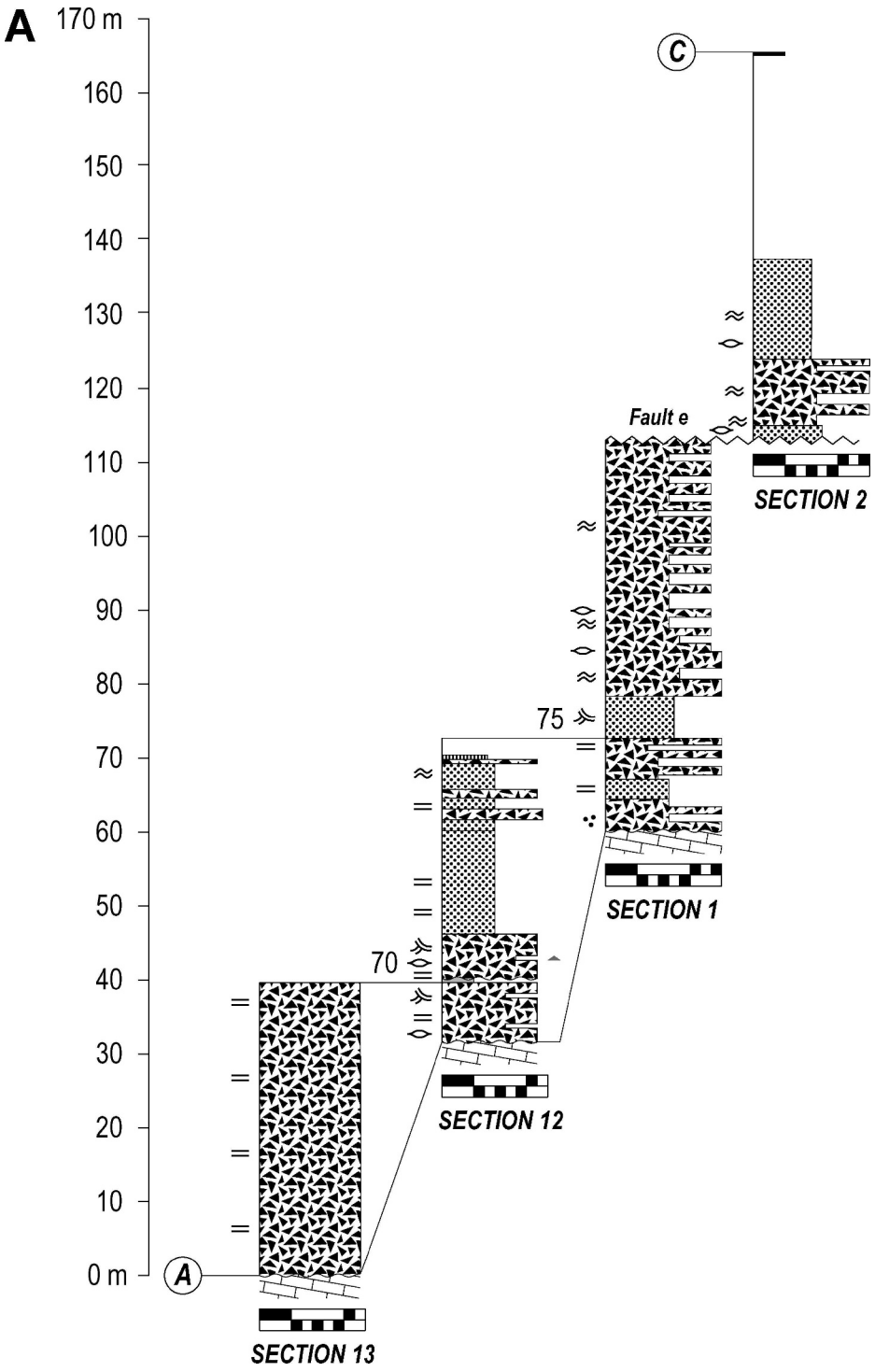

FIG. 5.—Stratigraphic sections through Eagle Mountain Formation at Eagle Mountain: **A)** basal breccia and sandstone interval; **B)** lower lacustrine and middle fluvial–lacustrine intervals (separated by surface C); **C)** upper lacustrine interval. Inset at lower right in Part B summarizes correlations. See Figure 3B for locations of sections. Columns are correlated using physical stratigraphic surfaces, with surfaces K, M, and P as well as sandstone and tuffaceous beds in sections 1, 12, and 13 selected as datums. Surface C was also used as datum to determine the vertical distance between sections 2 and 3. Dashed lines indicate uncertainty in correlation. Erosional relief depicted on surface J in sections 7 and 8 is schematic; the surface cuts up and down section at several places. Erosional contact on surface B in section 3 corresponds with the base of a lacustrine turbidite sandstone. Approximate distances between sections are given in meters at specific stratigraphic levels. Fault contacts without gaps represent an unknown amount of missing section, with the exception of fault d in section 4. Thicknesses of sections omitted or repeated by faults are determined by correlation of datums, except for the stratigraphy repeated in section 4 and omitted in section 11, which is based on field estimates of stratigraphic separation on faults d, h, and i. Other gaps in sections represent cover, and are inferred to be mostly siltstone. The grain size depicted represents average grain size for siltstone and sandstone beds, and average size of granule-size or larger clasts in the case of conglomerate and breccia beds (Wentworth scale). Some of the breccia and conglomerate includes abundant sandstone interbeds that are too thin to depict individually; those interbeds are shown schematically as fewer thicker units that still accurately convey the relative abundances of sandstone and breccia/conglomerate. To distinguish these schematic interbeds from actual measured sandstone beds, the schematic beds are shaded with the same fill as the surrounding conglomerate or breccia. Units thin enough that their lithology-coded fills may not be clear in the figure include the following: ash at ~ 40 m in section 12; carbonate beds just below surface E in section 7 and surfaces C, D, E, and H in section 8; carbonate beds at ~ 315 and ~ 320 m in section 4, ~ 325 and ~ 340 m in section 10, ~ 290 m in section 11, and ~ 70 m in section 12; very fine-grained sandstone ~ 85 and ~ 100 m in section 1; and conglomerate beds in section 3 just above surface D and above the additional surface traced to section 5 between surfaces C and D.

dispersion. Paleocurrents vary from approximately southward or southeastward in the third interval (below surface K) to approximately eastward above it (Fig. 6B). No systematic lateral variations emerge from the data. Tectonic tilt was removed by rotating each paleocurrent measurement manually on a stereonet, taking paleohorizontal from the attitudes of appropriate nearby beds (e.g., parallel-laminated siltstone or very fine-grained sandstone). For paleocurrents measured in bedding-plane view, the precision of the tilt correction was refined slightly by recalculating it via spherical trigonometry.

Basal Unconformity

The prominent unconformity underlying the Eagle Mountain Formation (surface A in Figures 3 and 5) displays at least ~ 110–140 m of erosional relief, the estimated maximum thickness of the basal breccia and sandstone unit. Uncertainty in this estimate derives from measuring and correlating sections 13, 12, and 1 on a dip slope; from minor stratigraphic repetition between sections 1 and 2 (fault e in Figure 3B); and from the covered interval between sections 2 and 3. Miller and Prave

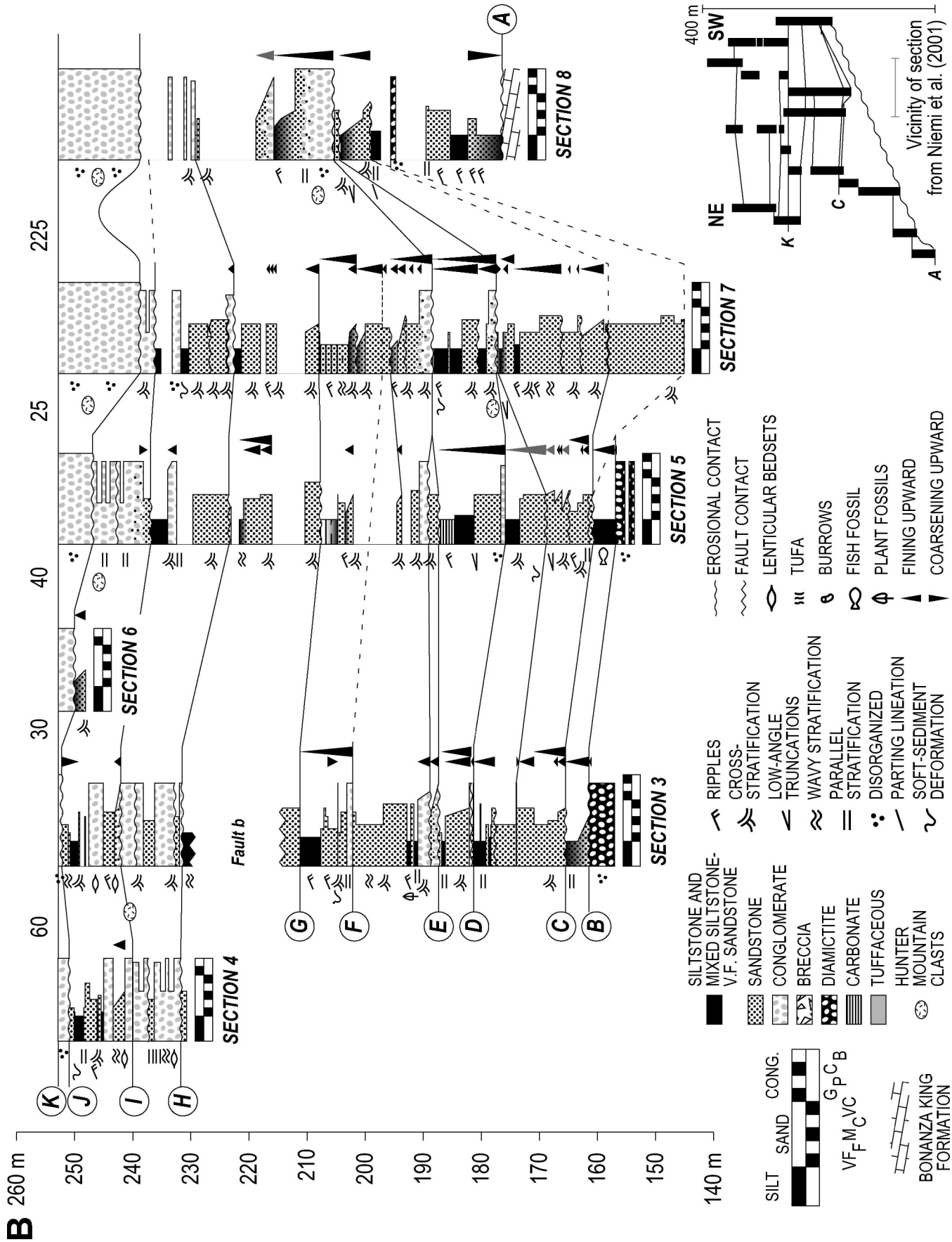

FIG. 5.—Continued.

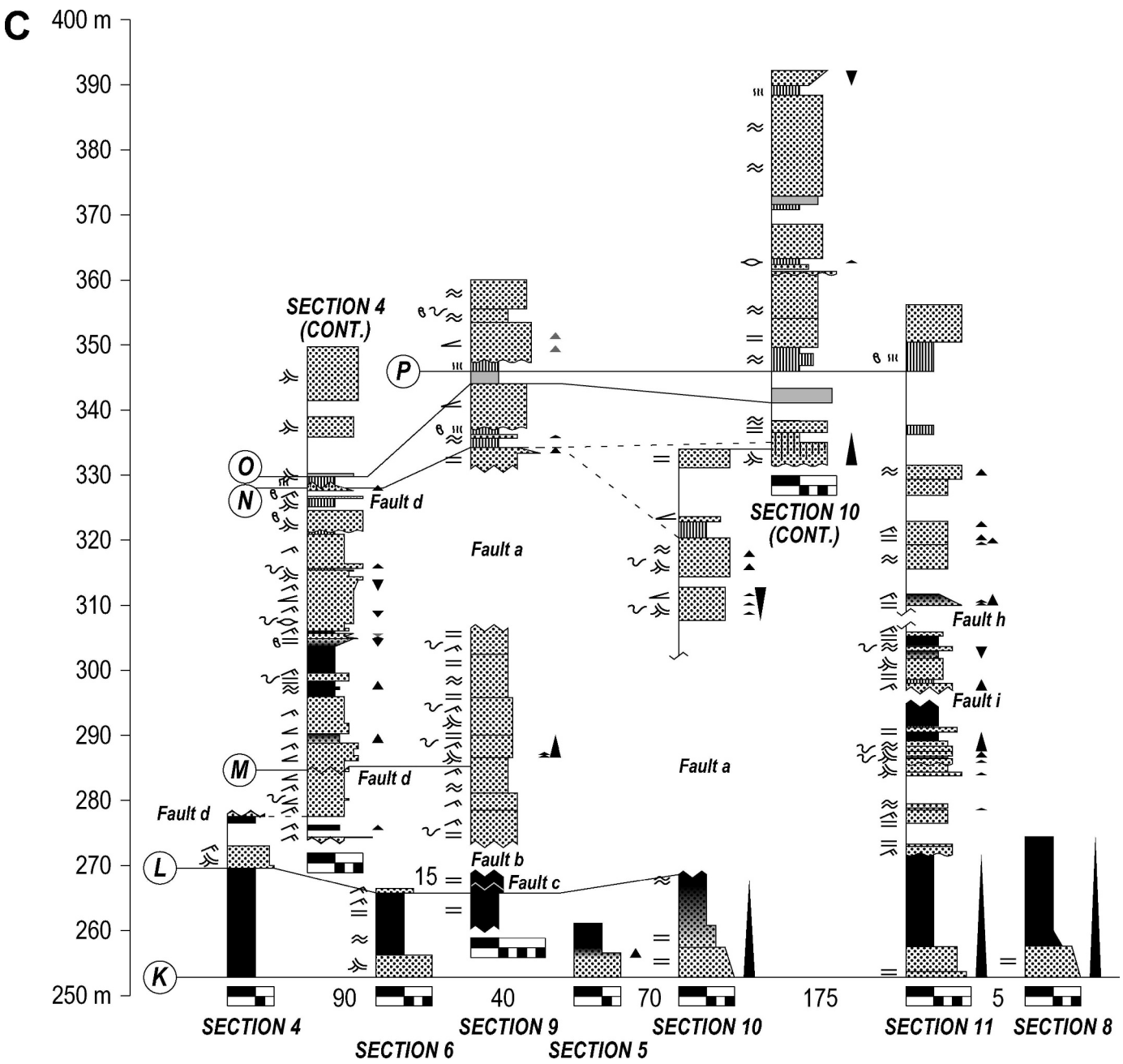

FIG. 5.—Continued.

(2002) showed that correlative strata near Furnace Creek Wash were similarly "deposited on a paleotopography that had several tens to many tens of meters of relief" (p. 848).

Although the orientation of the unconformity at Eagle Mountain cannot be measured directly in available outcrop, a paleotopographic slope dipping approximately either north-northeast or west-northwest is compatible with the stratigraphic thickening of the breccia–sandstone unit (Figs. 3B, 5A). Paleocurrent indicators in that unit are too scarce to rule out either orientation. In both cases, the implied mean paleogradient is $\sim 20^{\circ}$. That is sufficiently steep to account for local derivation of the breccia by mass wasting. The paleogradient is also consistent with the gradients of both modern and ancient bedrock valley walls (e.g., Christie-Blick et al. 1990; Hartshorn et al. 2002; Kale and Hire 2004; Schlunegger and Schneider 2005). The possibility that the basal relief of the Eagle Mountain Formation represents one wall of a paleovalley is illustrated conceptually in Figure 7. Details of the larger-scale paleotopography cannot be determined. Of the two hypothesized paleoslope directions, north-northeast is inconsistent with the presence of Cambrian carbonate rocks stratigraphically beneath thin Eagle Mountain breccia in the vicinity of section 2 (Fig. 3B). Therefore, a west-northwestward slope is regarded as more likely.

While erosional topography is sufficient to account for the local derivation and disorganized character of the basal breccia, we cannot exclude a role also for mass wasting from fault-related topography. In that case, the breccia may indicate proximity to a fault (to the west-northwest) and not only the mantling of erosional relief. No such fault or

evidence for concomitant stratigraphic growth is preserved today, and after 11.6 Ma, the Eagle Mountain Formation was evidently tilted in the opposite direction (to the east-southeast).

Cambrian bedding in the vicinity of the basal contact is estimated to have dipped ~ 17–18° southeastward immediately prior to Miocene sedimentation. This figure was calculated via a simple tilt correction using the Stereonet program of R.W. Allmendinger (http://www.geo.cornell.edu/geology/faculty/RWA/maintext.html). Breccia and sandstone in the lower part of the Eagle Mountain Formation are thought not to have experienced much differential compaction. Given that deposition was contemporaneous with the earliest phase of middle Miocene extension, we infer that the discordance between Cambrian and Miocene strata is due principally to late Paleozoic to Mesozoic compressional deformation. Paleozoic rocks as young as Mississippian and Pennsylvanian are present in the nearby Funeral and Nopah Ranges, respectively (Burchfiel et al. 1982; Çemen et al. 1985). So the depositional contact between the Eagle Mountain Formation and rocks as old as Cambrian, observed at each of its exposures, is also consistent with the development of marked erosional relief within the late Paleozoic to Mesozoic orogen.

Facies

Seven characteristic facies are found at Eagle Mountain: breccia and associated sandstone, conglomerate, cross-stratified sandstone, fine-grained sandstone and siltstone, diamictite, carbonate, and ash. Their distribution is illustrated in Figure 8, with the exception of the breccia and associated sandstone facies, which is found only in the lower part of the succession (Fig. 5A). The fine-grained facies and carbonate are predominant immediately below surface C and above surface K (Figs. 5B, C, 8); conglomerate and cross-stratified sandstone are most abundant between these surfaces. The data underpinning our descriptions of lithology, sedimentary structures, and paleocurrents are presented in Figures 5 and 6.

The breccia and associated sandstone consists of a mixture of angular to very angular Bonanza King carbonate pebbles and cobbles (with rare boulders) and coarse- to very fine-grained, poorly sorted siliciclastic sandstone (Fig. 9A). Carbonate-rich siltstone granules and pebbles are concentrated in isolated sandstone intervals a few centimeters thick. The breccia is coarsest and most abundant at the base of the section, with clast abundance as high as ~ 80% in sections 12 and 13 and ~ 30–50% in sections 1 and 2. Otherwise, no systematic grain-size trends are observed. Much of the facies is diffusely wavy- to parallel-stratified, but well developed cross-stratification is found in both breccia (Fig. 9B) and sandstone (Fig. 9C). Beds are centimeters to tens of centimeters thick, and locally channelized. Paleocurrent data are sparse and of uncertain significance. Geometrical reasoning suggests that paleoflow was predominantly towards the south-southwest along a hypothesized bedrock valley (Fig. 7), approximately parallel to the tilt-corrected strike of basal topography. The sense of flow is not constrained by such reasoning but is inferred by comparison with paleocurrent data from within the Eagle Mountain succession.

The conglomerate facies is characterized mainly by rounded pebbles and both framework- and matrix-support varieties. Sandstone interbeds are present in places (Fig. 9E). The facies is increasingly abundant, clast-rich, and coarse upsection; the uppermost unit (above surface J in Figure 10) is framework-supported and cobble-dominated, with rare boulders. At a smaller scale, conglomerate is associated with sandstone and siltstone facies in a systematic pattern of upward-fining units between surfaces C and K (Fig. 5B). Clast compositions include (in order of abundance) Bonanza King carbonate; quartzite of various colors; intraformational sandstone, siltstone, and carbonate; white marble; carbonate bearing crinoids, fusulinids, and corals, as well as dark dolomite that smells oily when freshly fractured; Hunter Mountain leucomonzogabbro; and metamorphosed igneous rocks. The Hunter Mountain clasts are extremely well rounded, even as boulders. The facies is typically channelized, and parallel-stratified to disorganized; some is cross-stratified. Beds are typically centimeters to tens of centimeters thick, and as much as several meters thick in amalgamated beds above the level of surface J. Tilt-corrected paleoflow was predominantly to the southeast, as indicated by channels (the most abundant paleocurrent indicator), scours, and grooves, as well as cross-stratification in associated sandstone (Fig. 6). The trend of exhumed erosional relief at surface J between sections 5 and 7 (Figs. 4, 10) is best estimated as 179° (laser range finder data), subparallel to the inferred paleostrike of the basal unconformity.

The cross-stratified sandstone facies is very coarse- to fine-grained, mainly moderately to poorly sorted, and granular or pebbly in places. It is typically channelized, and associated with conglomerate, fine-grained sandstone, and siltstone in systematic fining-upward units between surfaces C and K. Trough cross-strata are generally at angle of repose and centimeters to several tens of centimeters thick (Fig. 9D). They are the most common paleocurrent indicators, and they suggest that tilt-corrected paleoflow was predominantly to the southeast (Fig. 6). Current ripples are consistent with this direction. Paleoflow is also documented to the southeast or northwest by channels and grooves, and to the south-southwest by tabular cross-strata.

The siltstone and fine-grained sandstone facies is moderately to very well sorted, with rare granules and pebbles of carbonate-rich siltstone. Systematic grain-size trends are uncommon below surface C and above surface K, with the exception of upward fining in event layers. The facies is associated with diamictite and ash below surface C; with carbonate and ash above surface K; and with conglomerate, cross-stratified sandstone, and carbonate between surfaces C and K in a systematic pattern of fining-upward units. Beds are commonly parallel- and wavy-laminated. Other structures include current ripples, low-angle truncations, cross-stratification, and rare wave or hybrid current–wave ripples and climbing ripples. Turbidites up to a few centimeters thick are present below surface C at section 3. Event layers a few tens of centimeters thick are also found, characterized by sharp bases (some with sole marks), normal grading, and upward transitions from parallel laminae to low-angle cross-laminae or current ripples (Fig. 9F). Load structures, other evidence for soft-sediment deformation, and burrows are found both below surface C and above surface K, and less commonly between them. Fossils include a centimeters-long fish fossil (teleost) below surface C near section 5, as well as plants at a single locality between surfaces E and F near section 3. Tilt-corrected paleoflow is southward below surface C, and eastward with northeast–southwest wave motion above surface K. Specifically, paleoflow is shown to the east-southeast by current ripples (which provide most of the data), to the east by trough-cross-stratification, and to the south-southeast or north-northwest by scours, grooves, and parting lineation.

The diamictite facies is a disorganized mixture of a silt-dominated matrix and clasts of widely varying size. The term "diamictite" is used in its intended descriptive sense (Flint et al. 1960a, 1960b), with no glacial connotations. Clasts present in variable proportions consist of poorly sorted intraformational siltstone, sandstone, and carbonate (granules to angular, $>$ 1 m boulders), and extraformational types comparable to those in overlying conglomerate (pebbles). Clast abundance ranges from 5% to 45%, and winnowed lags locally cap the unit. The facies is associated with siltstone and fine-grained sandstone.

The carbonate facies is typically mudstone and includes both limestone and dolomite. It is silty to sandy in places and is associated with fine-grained sandstone and siltstone. It has local silicified nodules and possible thrombolites above surface K. It is massive to laminated, and includes local tufa above surface K.

The ash facies is white to pale green, distinctively low-density, clay- to coarse-sand-size pyroclastic fall, some with calcite cement (Niemi et al.

2001; major oxide composition from the same paper is detailed in Geological Society of America Data Repository item 2001031, http://www.geosociety.org/pubs/ft2001.htm). The material is unstratified to crudely parallel-stratified, and rarely diffusely cross-stratified. It forms lenses in the lower part of the succession. It is apparently more laterally continuous higher in the section but is rarely well exposed there.

In collecting the paleocurrent data summarized here and in Figure 6, there is obviously a tradeoff between obtaining sufficient observations for statistical significance and measuring only those features for which orientation can be confidently interpreted. The best indicators are those measurable on either the tops or bases of beds (the traces of trough cross-stratification, ripples, scours, and grooves). Measurements of channels, scours, and cross-stratification in cross section tend to bias results in favor of paleoflow directions parallel to the outcrop (south-southwest), even though measurements focused on relatively three-dimensional exposures. Otherwise, no clear-cut differences between indicators were found.

Stratigraphic Architecture

The Eagle Mountain Formation at Eagle Mountain is characterized by a series of mappable stratigraphic discontinuities. The most prominent, erosion surfaces C through J in Figures 3B, 4, and 5B, are associated with abrupt upward coarsening from siltstone or carbonate to conglomerate and sandstone, and with local relief of up to several meters. The greatest relief is present at surface J (~ 14 m; Fig. 10) and at surface C (~ 15 m inferred in the vicinity of section 7; Fig. 5B). Surfaces K and N are characterized by concordance and by abrupt upward fining (Fig. 5C). Additional, generally less distinctive surfaces were mapped to refine correlations between measured sections (Figs. 3, 5).

Lateral thickening towards the north-northeast between surfaces C and G (Figs. 3, 5B) is thought to represent a combination of stratigraphic growth and relief on successive erosion surfaces. Thickness variations are recognized at several levels within that interval, and with reference to a distinctive diamictite marker (at horizon B in Figure 5B). Any fault responsible for the inferred growth would have been located north of the present outcrop of the Eagle Mountain Formation, with an approximately east-southeast strike. That is approximately parallel to the Furnace Creek fault zone and transverse to the relief against which the lower part of the formation is inferred to have been deposited.

All of the coarse-grained facies between surfaces A and K display lenticularity at scales of tens of meters to a fraction of a meter. Channels are abundant between surfaces C and K, and are present locally in the basal breccia and sandstone (Figs. 5A, 9A). An example of crosscutting relationships among erosional surfaces in cross-stratified sandstone is detailed in Figure 11. In contrast, fine-grained facies tend to be both laterally continuous and tabular, exemplified by the sandstone and siltstone overlying surface K (Fig. 5C) and the siltstone and minor sandstone immediately underlying surface C (Fig. 5B).

Patterns of Grain-Size Variation

Systematic patterns of grain-size variation are observed primarily between surfaces C and K. Upward fining is present at the scale of beds, individual channels, and particularly the intervals between mapped erosion surfaces (Figs. 5B, 12). It is expressed in the full range of lithology, from conglomerate to siltstone, as well as in matrix, clast size, clast abundance, and relative thickness of coarse and fine layers. Fining is commonly accompanied by improved sorting of matrix (assessed visually following Tucker 1996), thinning of beds, and a transition from trough cross-stratification to current ripples. At the largest scale, and as noted above, the succession coarsens upward from below surface C to surface K. Within that interval, conglomerate becomes more abundant, thicker-bedded, more disorganized, and coarser-grained upwards.

PALEOENVIRONMENTAL INTERPRETATION

The evidence at hand indicates that the lower 60% of the Eagle Mountain Formation at Eagle Mountain (the portion below surface K) accumulated mainly in a fluvial or fluvially influenced setting rather than at an alluvial fan. That part of the succession specifically includes the interval known to contain Hunter Mountain batholith clasts, which for that reason is critical to the provenance argument supporting large-scale extension between Eagle Mountain and the Cottonwood Mountains. A braided fluvial interpretation for the interval between surfaces C and K is supported by the ubiquitous development of laterally persistent erosion surfaces, nested channels and trough cross-stratification, upward fining at the same range of scales, and the abundance of well-rounded clasts (e.g., Rust 1972; Smith 1974, 1990; Campbell 1976; Cant and Walker 1976; Cant 1978; Kraus 1984; Rust and Koster 1984; Miall 1985; Blair 1987b; Willis 1993; Blair and McPherson 1994a; Levy et al. 1994; Collinson 1996). Siltstone and carbonate found immediately beneath surfaces D, E, and G to J represent intervals of reduced discharge, local channel tops, or perhaps short-lived lake development.

Paleocurrent data are generally consistent with data obtained by Wright et al. (1999) at the Furnace Creek Wash locality (FC in Figure 1), and their scatter is largely attributable to the intrinsic spatial and temporal variability in a river system (e.g., Rust 1972; Willis 1993). This includes a combination of lateral and downstream accretion, as well as large-scale features (e.g., incised valleys and channels) representing

→

Fig. 6.—Paleocurrents from Eagle Mountain Formation at Eagle Mountain. **A)** Paleocurrent directions keyed to measured stratigraphic sections and an additional transect. Arrows represent best estimate of paleoflow at a given stratigraphic level in each section. Lateral distances between sections or between segments of individual sections (in meters, numbers in italics) are not to scale. Numbers below specific measurements indicate distance from nearest section in meters. Most arrows represent individual measurements, some of which are the best estimates from nearby measurements; other arrows represent averages of several measurements. All of the data are shown in Parts B and C. **B)** Vertical distribution of paleocurrents in meters, with respect to base of section 13. Note break in vertical axis between 60 m and 140 m. Solid vertical lines represent circular means of data for which sense of flow is known, calculated for the inferred fluvial interval bearing the Hunter Mountain clasts and for overlying and underlying lacustrine intervals. Note that lacustrine data below surface C in section 8 plot at the same elevation as some fluvial data above surface C in other sections. Measurements for which the sense of flow is not known are shown as two points (180° apart), with a black symbol for the point within 180° of the cross-strata mean and a gray symbol for the other. For symmetrical ripples and for channels in basal breccia and sandstone, circular means are shown by two dashed lines, and the black and gray symbols are divided by proximity to those lines. Laser range-finder measurement (diamond) is from surface J. **C)** Paleocurrent directions and circular means separated by type of paleocurrent indicator and by vertical interval. Means and standard deviations were calculated following Mardia (1972), after separating the indicators specifying sense of flow from those that do not. In each rose diagram, *n* is number of measurements and "bin max" is the greatest number of measurements in a single 10° bin. The radius of each shaded slice is proportional to the square root of the number of measurements in a bin. (Area scales with number of measurements.) Bins are defined so that a measurement of 20°, for example, falls into a 20–29° bin, not an 11–20° bin. Mean and standard deviation for all data in each plot are shown by black arrow and gray arc. Means for specific vertical intervals are shown by the white arrows. "HM" refers to the mostly fluvial interval containing Hunter Mountain clasts. Interval-specific means are not shown for rose diagrams in which all data are from a single interval or for measurements of trough cross-strata in cross section, for which only a single measurement (directed 090°) was made outside the "fluvial (HM)" interval (in the "lower lacustrine" interval). There is only a single measurement from parting lineations (136°/316°, in the "lower lacustrine" interval), and it is the only measurement from that interval in the "sense of flow unknown" diagram.

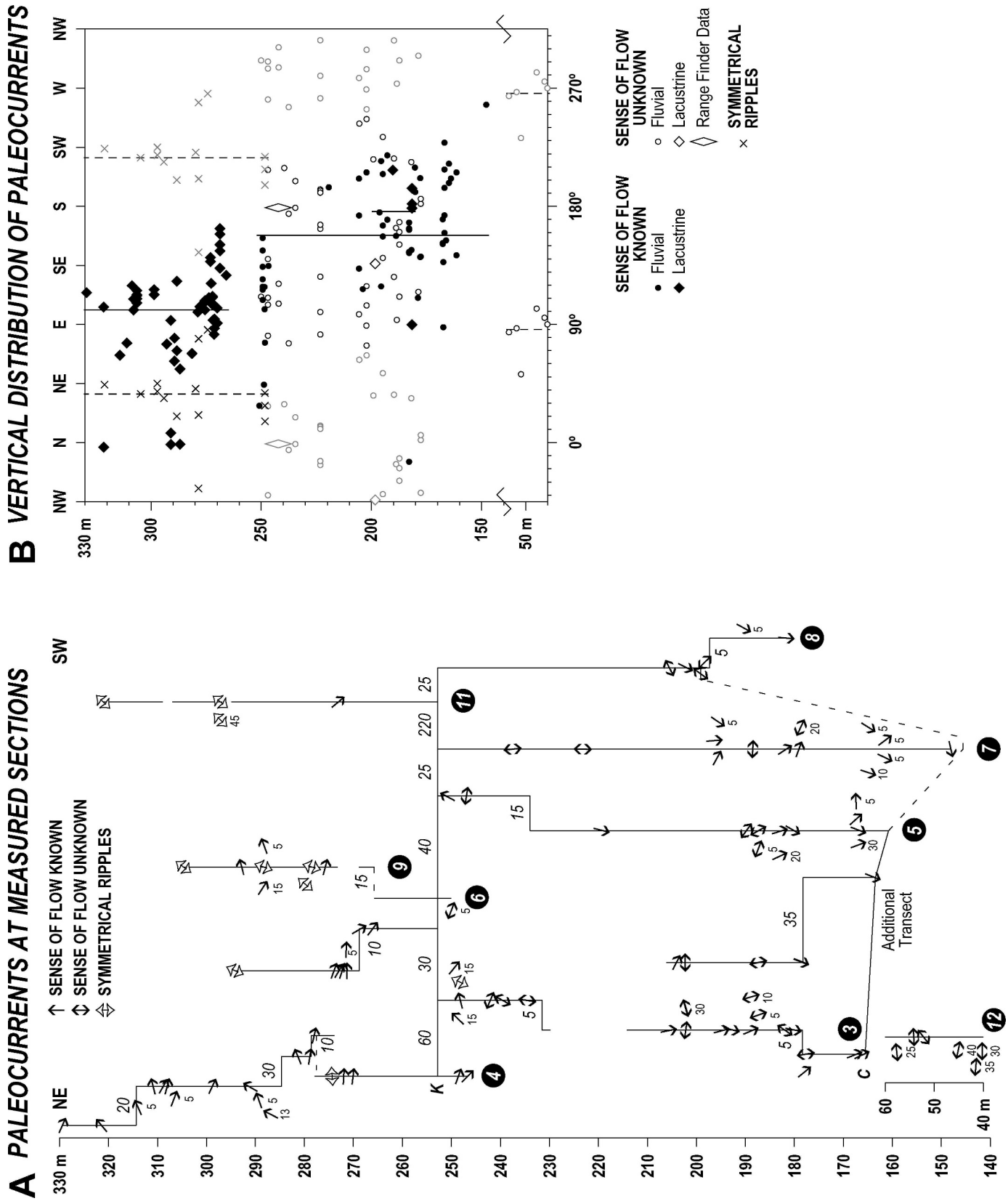
A PALEOCURRENTS AT MEASURED SECTIONS
NE
SW
SENSE OF FLOW KNOWN
SENSE OF FLOW UNKNOWN
SYMMETRICAL RIPPLES
330 m
320
310
300
290
280
270
260
250
240
230
220
210
200
190
180
170
160
150
140
K
C
Additional Transect
60
50
40 m
B VERTICAL DISTRIBUTION OF PALEOCURRENTS
NW
N
NE
E
SE
S
SW
W
NW
0°
90°
180°
270°
330 m
300
250
200
150
50 m
SENSE OF FLOW KNOWN
Fluvial
Lacustrine
SENSE OF FLOW UNKNOWN
Fluvial
Lacustrine
Range Finder Data
SYMMETRICAL RIPPLES

C PALEOCURRENTS BY INTERVAL AND INDICATOR

SENSE OF FLOW KNOWN

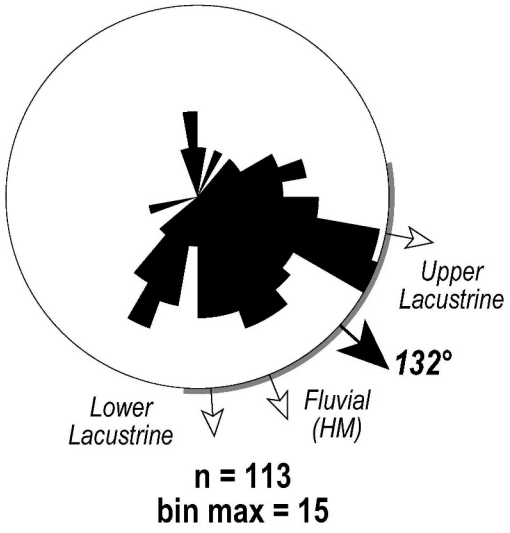

SENSE OF FLOW UNKNOWN

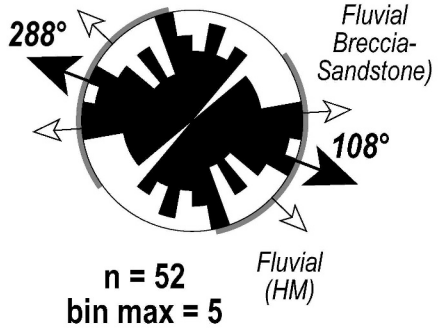

CROSS-STRATA

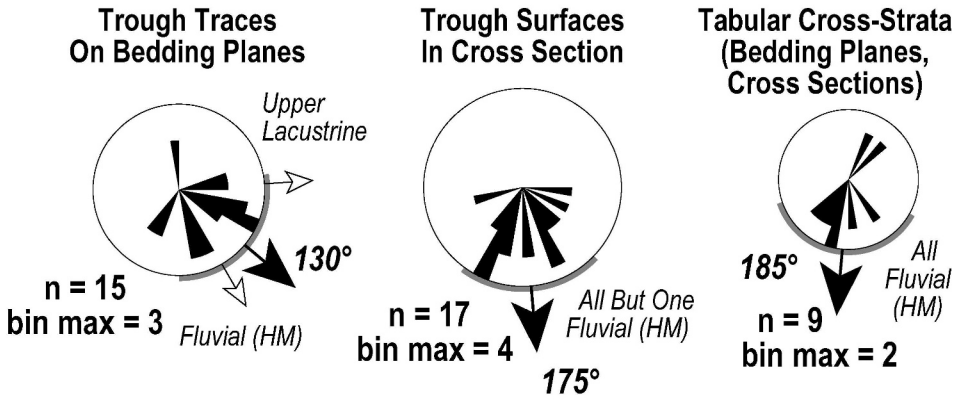

CURRENT RIPPLES

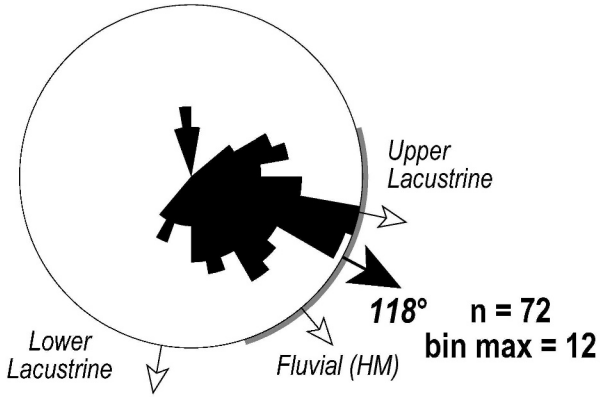

SYMMETRICAL RIPPLES

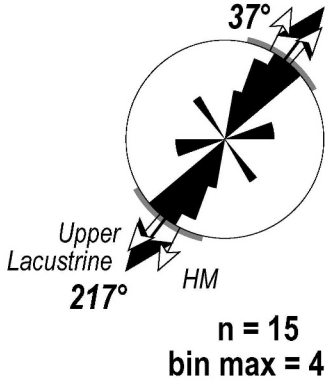

CHANNELS, SCOURS, AND GROOVES

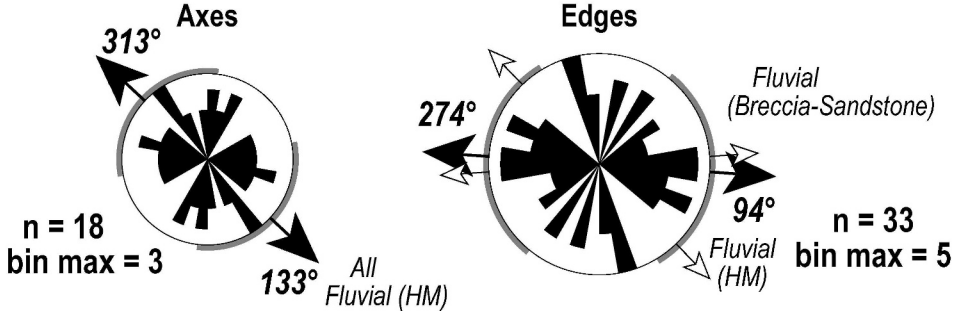

FIG. 6.—Continued.

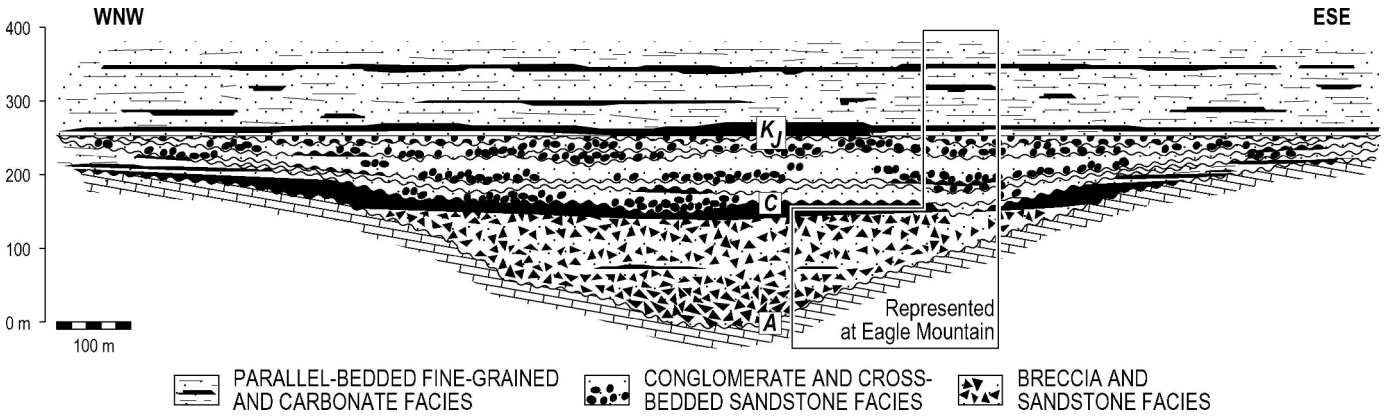

FIG. 7.—Conceptual cross section of Eagle Mountain Formation showing hypothesized basal paleovalley, including possible lateral continuations of geology exposed at Eagle Mountain (indicated approximately by box). The paleodip of underlying Cambrian carbonate rocks is ~ 17–18° to the southeast.

integration over longer timescales than small-scale features (e.g., cross-stratification, scours, grooves, and current ripples).

The flow is consistent with a source of sediment in the Cottonwood Mountains to the west-northwest. Given the modest size of the Eagle Mountain outcrop, however, it is not possible to distinguish any regional pattern from features of local paleogeographic significance or the possible effects of vertical-axis rotation. The local significance of the data is to show that channels are mostly oblique to the north-northeast strike of the outcrop. This is relevant to the assessment of stratigraphic geometry because the perceived aspect ratio of any erosional feature (Figs. 4, 5B, 11) is strongly influenced by whether its exposure is predominantly cross-sectional or longitudinal.

The breccia–sandstone facies is also interpreted as fluvial or fluvially influenced, but with a mixing of far-traveled, siliciclastic sand and locally derived, angular clasts of carbonate from valley walls. This interpretation is supported by the presence of cross-stratification and smaller-scale channelization (Fig. 9A–C), although they are not as common as between surfaces C and K. It is also consistent with the erosional relief on surface A.

Fine-grained sandstone, siltstone, diamictite, and carbonate facies, best developed immediately below surface C and above surface K, are inferred to be lacustrine. This interpretation is supported by the generally fine grain size, abundant tabular event layers and local thin turbidites, load and soft-sediment foundering structures, tufa, and a fish fossil. Noble (1941) also found freshwater fish fossils in correlative strata near Furnace Creek Wash, although the correlation is not definitive because the precise stratigraphic level and geographic location of the fossils is unspecified. The abundance of sandstone, albeit mostly fine- to very fine-grained, as well as the presence of trough cross-stratification, wave ripples, and tufa are consistent with a relatively nearshore setting. In places, the event layers are reminiscent of delta front. Nonetheless, we did not find well-developed examples of coarsening- and thickening-upward successions in these intervals. It is also possible that the coarser and more commonly cross-bedded strata at the top of the section represent a return to fluvial conditions (Niemi et al. 2001), although thick carbonate units are still common. The limited outcrop there makes it difficult to evaluate this possibility in terms of stratigraphic architecture. Disorganized diamictite found at a single level beneath surface B (Fig. 5B) is thought to represent subaqueous mass wasting and mixing of fluvially derived extraformational clasts, intraformational siltstone and sandstone blocks, and lacustrine mud. Paleocurrents above surface K show considerable variability. This is inferred to reflect paleogeographic variations near the shoreline, variations in the trajectory of wind-driven currents, and the relatively low lake-floor gradient.

SIGNIFICANCE OF STRATIGRAPHIC DISCONTINUITIES

Most of the mapped stratigraphic discontinuities (C, D, and G–J) are characterized by erosional relief and abrupt upward coarsening, and in the case of surface C, by a change from confidently interpreted lacustrine siltstone, sandstone, and diamictite to fluvial conglomerate and sandstone. The lacustrine deposits at that level are inferred to have been subaerially exposed and incised. They do not shoal upwards into fluvial facies. Among possible origins for the inferred subaerial degradation are tectonic tilting, climatically induced lake-level changes, and, with the exception of surface C, reorganization of the fluvial system. We hypothesize that tectonic tilting in an extensional setting may have involved deepening and narrowing of a hydraulically closed lake against a basin-bounding normal fault, with concomitant subaerial erosion at updip locations (e.g., Schlische 1991). Climatically induced lake-level changes and fluvial reorganization are also plausible given that observed cyclicity between surfaces C and K is well within the Milankovitch timescale band for orbital forcing (< 100 ky on average; e.g., Hinnov 2000).

Surfaces K and N are different. They are more or less concordant with underlying and overlying strata and are characterized by upward fining from conglomerate to sandstone and siltstone (K) or a change from siliciclastic to carbonate sedimentation (N). Both tectonic and climatic explanations can again be contemplated for this marked deepening of the paleoenvironment.

COMPARISON WITH PREVIOUS INTERPRETATIONS

The paleoenvironmental interpretations presented in this paper depart significantly from those of Niemi et al. (2001) primarily because we have placed greater emphasis on stratal geometry, three-dimensional facies arrangements, and grain-size variations within discontinuity-bounded intervals (Fig. 8). The interpretations of Niemi et al. (2001) at Eagle Mountain are based on a single composite section (their table A1 and fig. 2), and on generalized outcrop-scale descriptions of lithology and sedimentary structures, without reference to the systematic patterns documented here in the critical interval containing Hunter Mountain clasts.

Disorganized and Parallel-Stratified Deposits

Disorganized breccia and conglomerate, found preferentially at the base of the Eagle Mountain Formation (Fig. 5A), between surfaces I and K, and locally between surfaces C and I (Figs. 5B, 8), display some of the features associated with mass-flow deposits. Much of the succession is

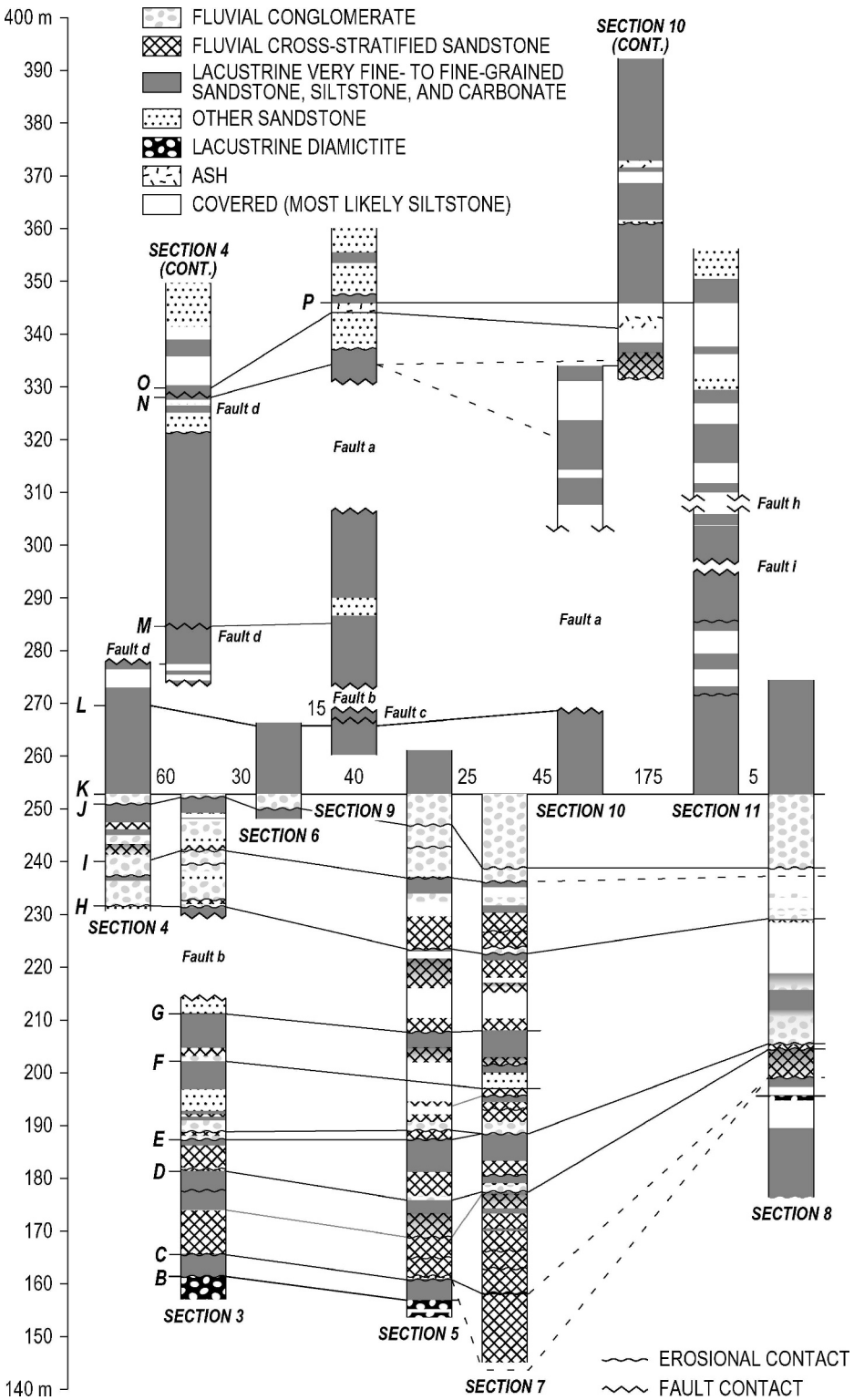

FIG. 8.—Distribution of facies at measured sections above the basal breccia–sandstone interval (modified from Figure 5). "Other sandstone" includes units that are insufficiently exposed to categorize with confidence or that are of transitional character.

well stratified, however. So the significance of disorganized beds is at best ambiguous.

Comparable disorganized and parallel-stratified conglomerate and sandstone as well as their unlithified equivalents have been documented in modern and ancient fluvial deposits, especially those in which deposition was accompanied by large fluctuations in discharge (e.g., Rust 1972; Smith 1974, 1990; Kraus 1984; Rust and Koster 1984; Levy et al. 1994; Collinson 1996). In the Eagle Mountain Formation, lithology varies more or less continuously between end members. We find little evidence for the "rhythmic" alternation (Blair 1999a, 2000) that is the hallmark of sheetflood couplets and sandskirts (e.g., Gloppen and Steel 1981; Blair and McPherson 1994a).

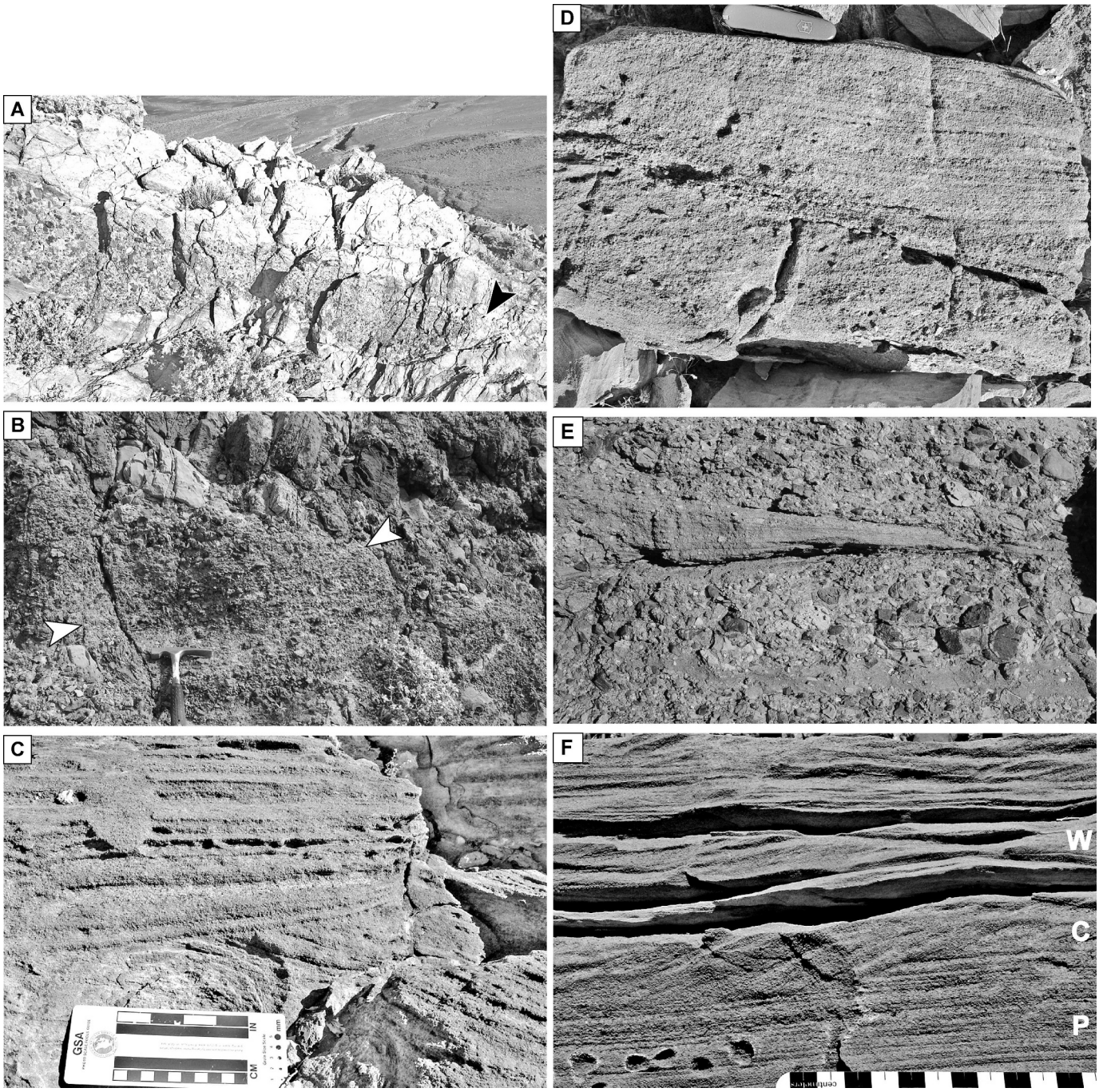

FIG. 9.—**A)** Lenticular, diffusely stratified breccia in basal breccia–sandstone unit. Arrowhead shows pinchout of lens. **B)** Cross-stratified breccia (~ 10 m from base of section 12). Arrowheads show orientation of cross-strata. **C)** Cross-stratified sandstone within breccia–sandstone facies (~ 15 m from base of section 1). Scale markings are inches at top and centimeters at bottom. **D)** Cross-stratified sandstone (near section 3). **E)** Conglomerate with interbedded sandstone (above surface I, section 3). **F)** Structures within inferred event layer above surface K: in stratigraphic order, these include parallel lamination (P), cross-lamination (C), and lower-relief, wavy lamination (W).

Clast Angularity

Angularity is similarly nondiagnostic or inconsistent with an alluvial-fan interpretation. Basal breccia clasts are angular and of local provenance because they were derived by mass wasting from sub-Miocene topography. Clasts in polymictic conglomerate at higher stratigraphic levels, especially clasts derived from the Hunter Mountain batholith, are generally well rounded. This contrasts with typical alluvial-fan deposits, and is consistent with deposition in a braided river. The marked change in the character of the Eagle Mountain Formation ~ 140 m above the base corresponds with the burial of erosional relief.

Cross-Stratification

The abundance of cross-stratification between surfaces C and K (Fig. 5B) is unexpected for alluvial fans. Alluvial fans are dominated by

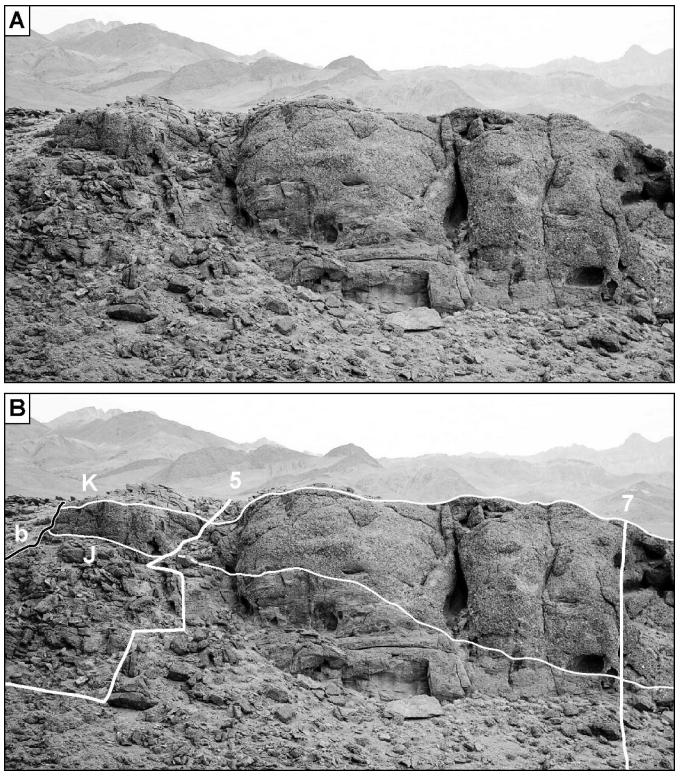

FIG. 10.— Large channel with ~ 14 m of relief: **A)** uninterpreted, and **B)** interpreted. Channel is located at surface J, in the vicinity of sections 5 and 7, and in the hanging wall of fault b. Abrupt transition to lacustrine interval at surface K is visible at top. Width of photographed area is ~ 40–50 m.

sheetfloods and debris flow (Blair and McPherson 1994a, 1994b; Els 1998), processes not normally associated with downstream-migrating bedforms. Cross-stratification is found in feeder valleys and associated channels (e.g., Gloppen and Steel 1981; Blair 1987b), but not over much of the fan surface.

Niemi et al. (2001) interpreted cross-stratification in the Eagle Mountain Formation as sheetflood antidunes. This was based on cross-strata dipping in the same direction (south to south-southwest) as "18 well-defined a–b plane fabrics from conglomerates" (p. 427). Clasts at Eagle Mountain, however, are typically equidimensional. In our experience, imbrication is both rare and not readily quantifiable. Our measurements of cross-strata and current ripples, as well as channels, scours, and grooves (Fig. 6), consistently provide no support for north-directed paleoflow. Most importantly, we find no evidence for the presence of antidunes. The geometry, scale, and abundance of the structures in question indicate that they formed under lower-flow-regime conditions (cf. Middleton 1965; Hand et al. 1969; Blair 1999a). This conclusion is unsurprising. Antidunes are poorly preserved in natural settings, and found mainly in association with parallel stratification (Simons and Richardson 1966; Hand et al. 1969; Blair 1987a, 1999a, 2000; Blair and McPherson 1994a).

Abundance of Channels

The fundamentally channelized geometry of coarse-grained deposits in the Eagle Mountain Formation is at odds with the unconfined nature of alluvial fans (e.g., Ballance 1984; Nemec et al. 1984; Smith 1990; Els 1998). Alluvial-fan deposits are typically sheetlike (e.g., Nemec et al. 1984; Rust and Koster 1984; Blair 1999b, 2000; Blair and McPherson 1994a; Martins-Neto 1996). Channels in steady-state fans are limited to feeder valleys; local erosional modifications of the fan surface, particularly through headward erosion from fault scarps; and/or a single trough that directs flows to the active part of the fan (Blair 1987a, 1999a, 1999b; Blair and McPherson 1994a, 1994b). The processes responsible for those channels do not result in net deposition, and "flows related to aggradation on fans invariably become unconfined" (Blair and McPherson 1994a, p. 454; Blair and McPherson 1994b; Blair 1999a).

Grain-Size Trends

The well-defined pattern between surfaces C and K—discontinuity-bounded upward fining at a scale of meters to tens of meters—is the opposite of that expected for steady-state fans: upward coarsening at multiple scales, resulting from radial progradation and lobe development (e.g., Steel et al. 1977; Heward 1978; Gloppen and Steel 1981; Rust and Koster 1984; Blair 1987a, 1987b; Gawthorpe et al. 1990; Gordon and Heller 1993; Dill 1995; Kemp 1996; López-Blanco et al. 2000; Clevis et al. 2003). Although upward fining can arise through lobe abandonment (e.g., Gloppen and Steel 1981; Martins-Neto 1996), it is unlikely to dominate the succession in the manner displayed by the Eagle Mountain Formation.

DISTANCE AND GRADIENT OF SEDIMENT TRANSPORT

If the deposits between surfaces C and K are predominantly fluvial, Hunter Mountain clasts as large as 1 m could have traveled several tens of kilometers or more from their source down a gradient of as little as a fraction of a degree (Blair and McPherson 1994a). Gravel as coarse as the Eagle Mountain conglomerate beds has traveled such distances along both modern and ancient rivers in orogenic to post-orogenic settings (the general state of the Death Valley area in the middle Miocene). Although the following examples may be diverse in catchment size, gradient, sediment caliber, discharge, climate seasonality and aridity, etc., they show that the coarseness of the Eagle Mountain clasts does not by itself preclude long-distance transport. Gravel-bed rivers sourced in the Southern Alps of New Zealand today span the entire Canterbury coastal plain—a distance of > 40 km in the case of the Waimakariri, which enters the Pacific Ocean north of Christchurch. Janecke et al. (2000) found pebble to boulder conglomerate "in most segments of the [Eocene] Lemhi Pass paleovalley," which is over 100 km long (p. 440). One tract of the paleovalley, with boulders < 3 m in diameter, is > 65 km from the nearest source. Clasts as large as boulders were transported > 100 km in a Paleogene braided river in Wyoming (Kraus 1984), and cobbles ~ 200–300 km in an Eocene river system in southern California (Steer and Abbott 1984). An Early Cretaceous river system in Wyoming, Utah, and Colorado distributed gravels over a distance of 600 km (Heller and Paola 1989).

River gradients of $< 0.5^\circ$ are sufficient to transport boulders for long distances in appropriate settings (Blair and McPherson 1994a). Cobbles > 20 cm are transported down the Waimakariri River, in New Zealand, from an elevation of 200 m to sea level at an average gradient of 0.26° (Land Information New Zealand 1997; N. Christie-Blick, unpublished observations). Modern Himalayan streams are somewhat steeper for distances of up to several tens of kilometers. The Bhagirath–Ganges and Tista Brahmaputra, for example, both have slopes $> 1^\circ$ for ~ 100 km (M.E. Brookfield 1998 and unpublished data; Lavé and Avouac 2001).

The overall conclusion to be drawn from these examples is not that the Eagle Mountain deposits represent any particular distance of transport or topographic slope. Neither the scale nor the character of the Miocene river system is well constrained, because available outcrop represents only a small erosional remnant of the original stratigraphy. The Himalaya and South Island, New Zealand, may also not be ideal analogues for a dissected orogen just beginning to undergo extensional deformation. Nor

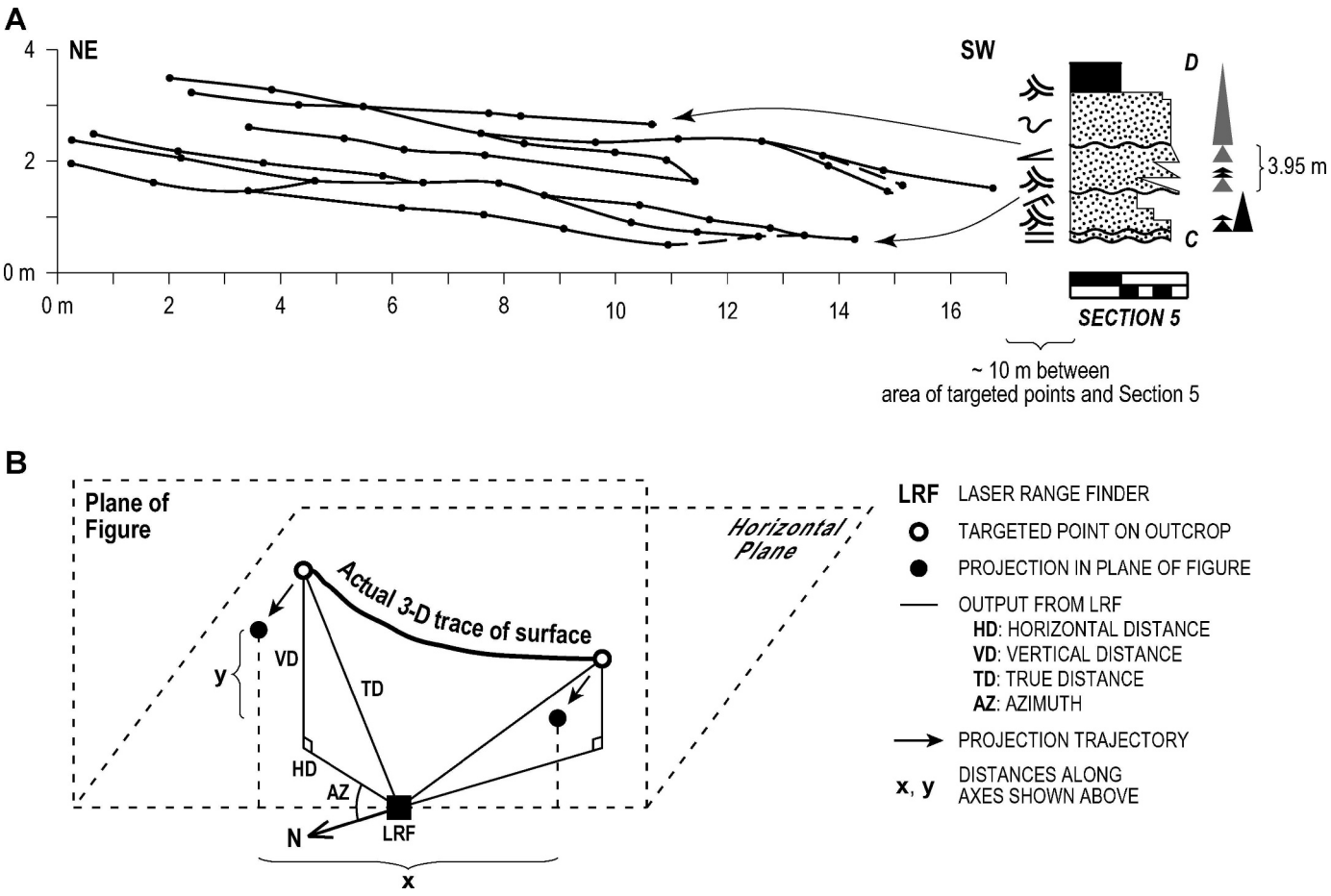

FIG. 11.—Cross cutting erosional surfaces ~ 10 m northeast of section 5, between surfaces C and D. **A)** Stratigraphic surfaces and correlative portion of section 5 indicated by arrows. Surfaces are defined by series of points located with a laser range finder (shown connected by smoothed lines). The exposure at Eagle Mountain subdues the aspect ratio of channels: the oblique view increases apparent channel width, and beds are tilted away from the observer on a gently sloping hillside, reducing apparent thickness as projected into a vertical plane. **B)** Method for projecting points. Vertical coordinate in Part A is equal to vertical distance reading from laser range finder. Horizontal coordinate in Part A is derived from horizontal distance, azimuth, and simple trigonometry, using outcrop azimuth of 027° for orientation of the figure plane.

are their high seasonal rainfall and discharge necessarily representative of the Eagle Mountain Formation. The significance of the quoted examples is that the presence of large clasts in the Eagle Mountain Formation does not by itself imply "proximal" sedimentation.

Niemi et al. (2001) recognized as much. Referring to both the local clustering of conglomerate clasts and the presence of plagioclase-rich sandstone in the Eagle Mountain Formation, they nevertheless found it "difficult to envisage a drainage system 100 km long that would consistently deliver coarse detritus from the southern Cottonwood Mountains to the Resting Spring Range without contamination from other parts of the drainage system" (p. 434). This assertion can be challenged on several grounds. (1) Much of the material in the Eagle Mountain Formation cannot be matched with a specific source, derived as it is from a Proterozoic–Paleozoic sedimentary wedge of regional scale. Although the remnants of that geology as well as other Cenozoic deposits vary between mountain ranges in the area today, the paleogeography in the middle Miocene is largely unconstrained. Little is known about the topography and drainage configuration at the time, as well as which rocks were exposed. (2) There is specifically no known source in the Cottonwood Mountains for metamorphosed igneous clasts observed at Eagle Mountain and in the Resting Spring Range outcrop. (3) Clustering of Hunter Mountain clasts is observed only locally in the Resting Spring Range exposure, and not at all at Eagle Mountain. Admittedly, the existence of any clustering is intriguing and its origin is not obvious. Nonetheless, it is explicable perhaps by rare mass wasting events in the vicinity of the batholith, a comparatively low sediment flux from tributaries (Rice 1998), or incomplete mixing of that sediment once it entered the main drainage (Bradley et al. 1972). Much depends on whether the streams involved were equilibrated (Cawood et al. 2003). Whatever the case may be, we do not think that clustering represents a sufficient basis for inferring that the Eagle Mountain Formation accumulated adjacent to the Hunter Mountain batholith. Given that there must have been some crustal extension across the Death Valley region, and conceivably quite a lot of extension, sediment transport need not have been as great as 100 km for Hunter Mountain material to be found today on the east side of the Resting Spring Range. It is also not necessary for transport in a river system to have exceeded the 20 km maximum advocated by Niemi et al. (2001). Our point is that the direction and magnitude of extension are unconstrained by the Eagle Mountain Formation. The distribution of Hunter Mountain clasts may instead represent the approximate locus of a proposed southeast-flowing mid-Miocene drainage, along what is modern-day Furnace Creek Wash and beyond (Çemen 1999; Wright et al. 1999). The decision by Niemi et al. (2001) to retain separate names for the Navadu and Eagle Mountain

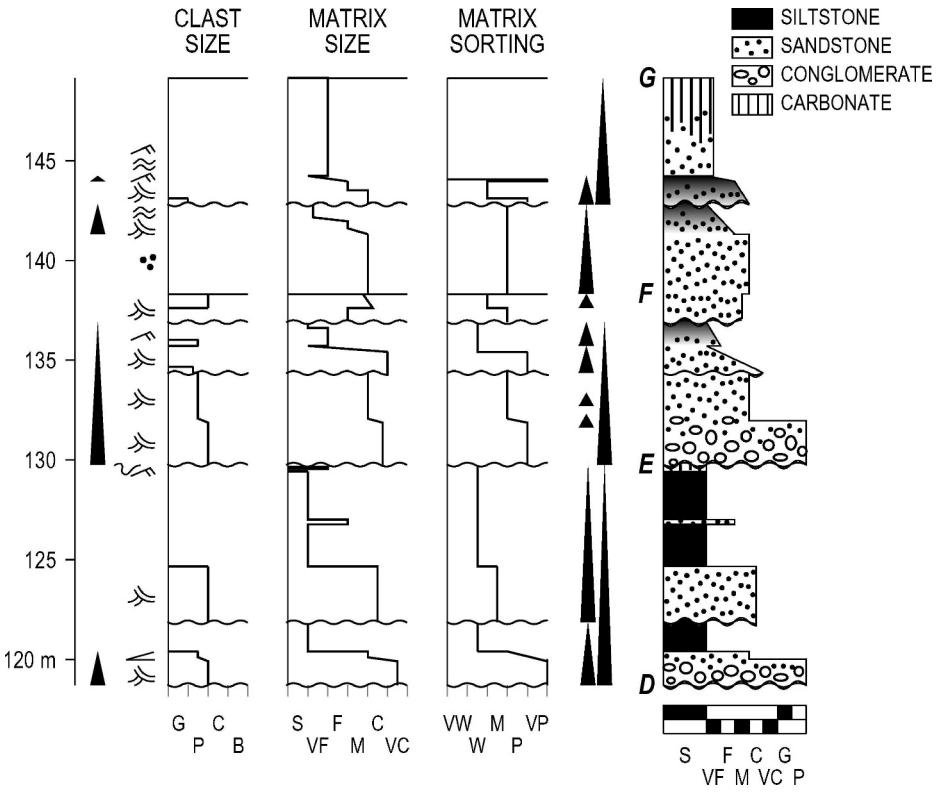

FIG. 12.—Detail of section 7 between surfaces D and G. Abbreviations on horizontal axis represent the Wentworth grain-size scale and "very well," "well," "moderate," "poor," and "very poor" for degree of sorting (assessed visually following Tucker 1996). Upward fining, manifested by decreasing clast size and matrix size, is accompanied by improved sorting, thinning of beds, and reduction in scale of sedimentary structures. Triangles show the various scales of these trends in grain size (right) and bedding (left). Carbonate underlies surface G.

formations was prescient, in retrospect, particularly their reasoning that the formations may have been deposited in separate settings.

LOCAL DEFORMATION

The Eagle Mountain Formation at Eagle Mountain is structurally simple. However, the presence of minor faults and folds and crosscutting conglomerate bodies influences perceptions of the overall succession, lateral relationships, and stratigraphic development. So these features are summarized briefly here, with details to appear elsewhere.

Normal, reversed normal, and oblique-slip faults cut the stratigraphy with up to 34 m of separation (Figs. 3, 5). They are characterized by fractures, breccia, possible gouge (now lithified), slickensides, and open folds centimeters to a few tens of centimeters in amplitude. The timing of faulting is not well constrained. Nonetheless, the lack of evidence for stratigraphic growth against or across mapped faults or for overlap by younger strata suggests that most or all of the deformation postdates deposition. Measured attitudes for faults vary, though with a preferred strike of either north or east-northeast after tilt correction. Most prominent in terms of offset and length are the reversed normal faults a and b (Fig. 3B). Anomalous compressional faults and folds observed in the vicinity of surface C south of section 8 (Fig. 3B) are of uncertain origin but perhaps are related to the nearby eastward termination of the Furnace Creek strike-slip fault zone (Fig. 1; Çemen et al. 1985; Wright et al. 1999; Snow and Wernicke 2000; Miller and Prave 2002).

Five irregularly shaped, internally disorganized, crosscutting bodies of pebble conglomerate (Fig. 3B) are inferred to represent tectonically induced fissures filled episodically from the top, as opposed to injections. This interpretation is supported by lithological similarities preferentially with overlying strata rather than underlying strata, and by locally developed internal layering. It is also difficult to account for the development of sufficient overpressure for the large-scale injection of gravel in an extensional tectonic setting, and in sandy sediments deposited on fully lithified carbonate rocks.

CONCLUSIONS

A sedimentological and stratigraphic re-evaluation of the middle Miocene Eagle Mountain Formation at Eagle Mountain, California, indicates that deposition took place in a fluvial–lacustrine setting. The result is important because the presence of clasts as large as boulders derived from the Hunter Mountain batholith of the Cottonwood Mountains, combined with an alluvial-fan interpretation for the conglomerate in which the clasts are found, has been regarded as providing definitive, independent support for long-hypothesized, large-scale crustal extension across the Death Valley region (e.g., Snow and Wernicke 2000). In particular, those findings were presented as corroborating the magnitude of extension suggested by structural reconstructions and as restricting the timing of it to post-11 Ma (Niemi et al. 2001). If the boulders were transported to their site of deposition by rivers, then deposition was not necessarily close to the source and subsequent tectonic transport cannot be discriminated. While our study has no direct bearing on the other evidence underpinning palinspastic reconstructions, those reconstructions involve inherent uncertainties in the correlation and pre-extensional configuration of markers that the Eagle Mountain piercing point appeared to circumvent. A definitive measure of extension across the central Death Valley corridor, then, depends on the resolution of existing ambiguities in the correlation of pre-extensional markers (e.g., Snow and Wernicke 2000) or on the recognition of demonstrably proximal sedimentary facies tectonically distributed across the region (e.g., Topping 1993).

Mineral cooling ages of Late Cretaceous age have been cited as evidence of extensional deformation in the Death Valley region at that time (e.g., Applegate and Hodges 1995); however, Oligocene strata in the Grapevine and Funeral mountains preserve the oldest unambiguous evidence of upper crustal deformation (e.g., Saylor 1991). Although extension may have begun locally as early as the Oligocene, predominantly late Miocene and younger deformation is consistent with patterns of tilting that are unchanged by a reinterpretation of the sedimentology of

the Eagle Mountain Formation. We hypothesize that prior to 11 Ma, locations in what are now northern Death Valley, Furnace Creek Wash, Eagle Mountain, and the eastern flank of the Resting Spring Range were connected by a throughgoing drainage.

Specific new conclusions for the Eagle Mountain locality include the following. (1) The Eagle Mountain Formation is preserved in part atop ~ 110–140 m of local topographic relief, possibly representing one wall of a valley now oriented approximately south-southwest. Monolithologic carbonate breccia that constitutes much of the fill represents local mass wasting, resedimented at least in part by fluvial processes. (2) Overlying fluvial–lacustrine deposits ~ 120 m thick—the interval in which Hunter Mountain clasts are observed—are subdivided by eight map-scale erosion surfaces, with as much as 15 m of local erosional relief. The existence of those surfaces, the prevalence of channelization and cross-stratification, the presence of systematic upward fining at a range of scales, and the predominance of rounded clasts in conglomerate provide the key evidence for the fluvial interpretation. Evidence for stratigraphic growth towards the north-northeast in this same interval, and referenced to the same surfaces, is consistent with the existence of a fault transverse to the possible basal paleovalley and north of available outcrop. Growth has not been recognized at other stratigraphic levels, or in association with mapped faults. (3) Paleocurrents are generally directed between southward and eastward, and not to the north and east, as previously reported. This conclusion is based on 180 measurements of cross-strata, ripples, and various erosional features. North-directed flow, inferred on the basis of clast imbrication and purported antidunes, is not consistent with our data. (4) The overall thickness of the Eagle Mountain Formation at Eagle Mountain is greater than previously thought (~ 400 m versus ~ 300 m). Much of the difference relates to the thicknesses of the basal breccia and an upper interval of mainly lacustrine sandstone and siltstone (also ~ 140 m). The revised estimate, based on several overlapping sections, also accounts for stratigraphic attenuation by previously unrecognized faults that cut obliquely through the outcrop.

ACKNOWLEDGMENTS

This research was completed with the support of a National Science Foundation Graduate Research Fellowship and a Geological Society of America Graduate Student Research Grant (to Renik). We acknowledge the Columbia University Department of Earth and Environmental Sciences for help with field expenses; the Seismology, Geology and Tectonophysics Division at Lamont-Doherty Earth Observatory for cost-sharing on the purchase of a laser range finder; Aero Tech Mapping of Las Vegas, Nevada, for timely acquisition of high-resolution aerial photographs; and the Oil and Natural Gas Corporation, Inc. (India) for a consulting contract. Christie-Blick acknowledges the Department of Geological Sciences at the University of Canterbury, New Zealand, for hospitality during his 2006–07 sabbatical leave. We thank Terence Blair, Jon Spencer, Jacqueline Huntoon, and Colin North for reviews of the manuscript and editorial advice; Michael Brookfield for sharing data on Himalayan rivers; Jessie Cherry, Bella Gordon, Simon Mayer, Abby Swann, Zachary Walke, and Robert Wallace for field assistance; Mark Anders, Jon Barbour, Ibrahim Çemen, Chris Fridrich, Karen Hanghøj, Peter Kelemen, Paul Olsen, Colin Stark, and Chris Walker for advice; and Darrel Cowan, Marli Miller, Terry Pavlis, and Laura Serpa for use of the SHEAR facility in Shoshone, California. Lamont-Doherty Earth Observatory Contribution Number 7102.

REFERENCES

Applegate, J.D.R., and Hodges, K.V., 1995, Mesozoic and Cenozoic extension recorded by metamorphic rocks in the Funeral Mountains, California: Geological Society of America, Bulletin, v. 107, p. 1063–1076.

Ballance, P.F., 1984, Sheet-flow-dominated gravel fans of the non-marine middle Cenozoic Simmler Formation, central California: Sedimentary Geology, v. 38, p. 337–359.

Blair, T.C., 1987a, Sedimentary processes, vertical stratification sequences, and geomorphology of the Roaring River alluvial fan, Rocky Mountain National Park, Colorado: Journal of Sedimentary Petrology, v. 57, p. 1–18.

Blair, T.C., 1987b, Tectonic and hydrologic controls on cyclic alluvial fan, fluvial, and lacustrine rift-basin sedimentation, Jurassic–lowermost Cretaceous Todos Santos Formation, Chiapas, Mexico: Journal of Sedimentary Petrology, v. 57, p. 845–862.

Blair, T.C., 1999a, Sedimentary processes and facies of the waterlaid Anvil Spring Canyon alluvial fan, Death Valley, California: Sedimentology, v. 46, p. 913–940.

Blair, T.C., 1999b, Sedimentology of the debris-flow-dominated Warm Spring Canyon alluvial fan, Death Valley, California: Sedimentology, v. 46, p. 941–965.

Blair, T.C., 2000, Sedimentology and progressive tectonic unconformities of the sheetflood-dominated Hell's Gate alluvial fan, Death Valley, California: Sedimentary Geology, v. 132, p. 233–262.

Blair, T.C., and McPherson, J.G., 1994a, Alluvial fans and their natural distinction from rivers based on morphology, hydraulic processes, sedimentary processes, and facies assemblages: Journal of Sedimentary Research, v. 64, p. 450–489.

Blair, T.C., and McPherson, J.G., 1994b, Alluvial fan processes and forms, *in* Abrahams, A.D., and Parsons, A.J., eds., Geomorphology of Desert Environments: London, Chapman & Hall, p. 354–402.

Bradley, W.C., Fahnestock, R.K., and Rowekamp, E.T., 1972, Coarse sediment transport by flood flows on Knik River, Alaska: Geological Society of America, Bulletin, v. 83, p. 1261–1284.

Brady, R.J., Wernicke, B.P., and Niemi, N.A., 2000, Reconstruction of Basin and Range extension and westward motion of the Sierra Nevada Block, *in* Lageson, D.R., Peters, S.G., and Lahren, M.M., eds., Great Basin and Sierra Nevada: Geological Society of America, Field Guide 2, p. 75–96.

Brookfield, M.E., 1998, The evolution of the great river systems of southern Asia during the Cenozoic India–Asia collision: rivers draining southwards: Geomorphology, v. 22, p. 285–312.

Burchfiel, B.C., Hamill, G.S., IV, and Wilhelms, D.E., 1982, Stratigraphy of the Montgomery Mountains and the northern half of the Nopah and Resting Spring Ranges, Nevada and California: Geological Society of America, Map and Chart Series, MC-44.

Burchfiel, B.C., Cowan, D.S., and Davis, G.A., 1992, Tectonic overview of the Cordilleran orogen in the western United States, *in* Burchfiel, B.C., Lipman, P.W., and Zoback, M.L., eds., The Cordilleran Orogen: Coterminous U.S.: Geological Society of America, The Geology of North America, v. G-3, p. 407–479.

Campbell, C.V., 1976, Reservoir geometry of a fluvial sheet sandstone: American Association of Petroleum Geologists, Bulletin, v. 60, p. 1009–1020.

Cant, D.J., 1978, Development of a facies model for sandy braided river sedimentation: Comparison of the South Saskatchewan River and the Battery Point Formation, *in* Miall, A.D., ed., Fluvial Sedimentology: Canadian Society of Petroleum Geologists, Memoir 5, p. 627–639.

Cant, D.J., and Walker, R.G., 1976, Development of a braided-fluvial facies model for the Devonian Battery Point Sandstone, Québec: Canadian Journal of Earth Sciences, v. 13, p. 102–119.

Cawood, P.A., Nemchin, A.A., Freeman, M., and Sircombe, K., 2003, Linking source and sedimentary basin: Detrital zircon record of sediment flux along a modern river system and implications for provenance studies: Earth and Planetary Science Letters, v. 210, p. 259–268.

Çemen, I., 1999, Tectonostratigraphic relationship between the Cenozoic sedimentary successions of the southern Funeral Mountains, Furnace Creek Basin, Eagle Mountain, and the north end of the Resting Spring Range: U.S. Geological Survey, Open-File Report 99-0153, p. 56–57.

Çemen, I., and Baucke, W., 2005, Magnitude of strike-slip displacement along the southern Death Valley–Furnace Creek fault zone, Death Valley, California (abstract): Geological Society of America, Annual Meeting, Abstracts with Programs, v. 37, p. 275.

Çemen, I., Wright, L.A., Drake, R.E., and Johnson, F.C., 1985, Cenozoic sedimentation and sequence of deformational events at the southeastern end of the Furnace Creek strike-slip fault zone, Death Valley region, California, *in* Biddle, K.T., and Christie-Blick, N., eds., Strike-Slip Deformation, Basin Formation, and Sedimentation: SEPM, Special Publication 37, p. 127–141.

Çemen, I., Wright, L.A., and Prave, A.R., 1999, Stratigraphic and tectonic implications of the latest Oligocene and early Miocene sedimentary succession, southernmost Funeral Mountains, Death Valley region, California, *in* Wright, L.A., and Troxel, B.W., eds., Cenozoic Basins of the Death Valley Region: Geological Society of America, Special Paper 333, p. 65–86.

Christie-Blick, N., von der Borch, C.C., and DiBona, P.A., 1990, Working hypotheses for the origin of the Wonoka Canyons (Neoproterozoic), South Australia: American Journal of Science, v. 290-A, p. 295–332.

Clevis, Q., de Boer, P., and Wachter, M., 2003, Numerical modelling of drainage basin evolution and three-dimensional alluvial fan stratigraphy: Sedimentary Geology, v. 163, p. 85–110.

Collinson, J.D., 1996, Alluvial sediments, *in* Reading, H.G., ed., Sedimentary Environments: Processes, Facies and Stratigraphy: Oxford, U.K., Blackwell Science, p. 37–82.

Corbett, K.P., 1990, Basin and Range extensional tectonics at the latitude of Las Vegas, Nevada: Discussion: Geological Society of America, Bulletin, v. 102, p. 267–268.

Czajkowski, J., 2002. Cretaceous contraction in the Lees Camp Anticline: Inyo Mine and vicinity, Funeral Mountains, Death Valley, California [M.S. thesis]: Eugene, University of Oregon, 73 p.

Czajkowski, J.L., and Miller, M.G., 2001, Cretaceous contraction in the Lees Camp Anticline: Inyo Mine and vicinity, Funeral Mountains, Death Valley, California (abstract): Geological Society of America, Annual Meeting, Abstracts with Programs, v. 33, 151 p.

Dill, H.G., 1995, Heavy mineral response to the progradation of an alluvial fan: implications concerning unroofing of source area, chemical weathering and palaeo-relief (Upper Cretaceous Parkstein fan complex, SE Germany): Sedimentary Geology, v. 95, p. 39–56.

Els, B.G., 1998, The question of alluvial fans in the auriferous Archaean and Proterozoic successions of South Africa: South African Journal of Geology, v. 101, p. 17–25.

Fanning, C.M., and Link, P.K., 2004, U-Pb SHRIMP ages of Neoproterozoic (Sturtian) glaciogenic Pocatello Formation, southeastern Idaho: Geology, v. 32, p. 881–884.

Flint, R.F., Sanders, J.E., and Rodgers, J., 1960a, Diamictite: a substitute term for symmictite: Geological Society of America, Bulletin, v. 71, p. 1809–1810.

Flint, R.F., Sanders, J.E., and Rodgers, J., 1960b, Symmictite: a name for nonsorted terrigenous sedimentary rocks that contain a wide range of particle sizes: Geological Society of America, Bulletin, v. 71, p. 507–510.

Gawthorpe, R.L., Hurst, J.M., and Sladen, C.P., 1990, Evolution of Miocene footwall-derived coarse-grained deltas, Gulf of Suez, Egypt: implications for exploration: American Association of Petroleum Geologists, Bulletin, v. 74, p. 1,077–1,086.

Gloppen, T.G., and Steel, R.J., 1981, The deposits, internal structure, and geometry in six alluvial fan–fan delta bodies (Devonian–Norway)—A study in the significance of bedding sequence in conglomerates, *in* Ethridge, F.G., and Flores, R.M., eds., Recent and Ancient Nonmarine Depositional Environments: Models for Exploration: SEPM, Special Publication 31, p. 49–69.

Gordon, I., and Heller, P.L., 1993, Evaluating major controls on basinal stratigraphy, Pine Valley, Nevada: Implications for syntectonic deposition: Geological Society of America, Bulletin, v. 105, p. 47–55.

Hand, B.M., Wessel, J.M., and Hayes, M.O., 1969, Antidunes in the Mount Toby Conglomerate (Triassic), Massachusetts: Journal of Sedimentary Petrology, v. 39, p. 1310–1316.

Hartshorn, K., Hovius, N., Dade, W.B., and Slingerland, R.L., 2002, Climate-driven bedrock incision in an active mountain belt: Science, v. 297, p. 2036–2038.

Heaman, L.M., and Grotzinger, J.P., 1992, 1.08 Ga diabase sills in the Pahrump Group, California: Implications for development of the Cordilleran miogeocline: Geology, v. 20, p. 637–640.

Heller, P.L., and Paola, C., 1989, The paradox of Lower Cretaceous gravels and the initiation of thrusting in the Sevier orogenic belt, United States Western Interior: Geological Society of America, Bulletin, v. 101, p. 864–875.

Heward, A.P., 1978, Alluvial fan sequence and megasequence models: with examples from Westphalian D—Stephanian B coalfields, northern Spain, *in* Miall, A.D., ed., Fluvial Sedimentology: Canadian Society of Petroleum Geologists, Memoir 5, p. 669–702.

Heydari, E., 1986, Geology of the Resting Spring Pass tuff, Inyo County, California: California Geology, v. 39, p. 253–261.

Hinnov, L.A., 2000, New perspectives on orbitally forced stratigraphy: Annual Review of Earth and Planetary Sciences, v. 28, p. 419–475.

Holm, D.K., and Wernicke, B., 1990, Black Mountains crustal section, Death Valley extended terrain, California: Geology, v. 18, p. 520–523.

Janecke, S.U., VanDenburg, C.J., Blankenau, J.J., and M'Gonigle, J.W., 2000, Long-distance longitudinal transport of gravel across the Cordilleran thrust belt of Montana and Idaho: Geology, v. 28, p. 439–442.

Jennings, C.W., Burnett, J.L., and Troxel, B.W., 1962. Geologic Map of California: Trona Sheet: Sacramento, California Department of Conservation, Division of Mines and Geology.

Kale, V.S., and Hire, P.S., 2004, Effectiveness of monsoon floods on the Tapi River, India: role of channel geometry and hydrologic regime: Geomorphology, v. 57, p. 275–291.

Kemp, J., 1996, The Kuara Formation (northern Arabian Shield); definition and interpretation: a probable fault-trough sedimentary succession: Journal of African Earth Sciences, v. 22, p. 507–523.

Kraus, M.J., 1984, Sedimentology and tectonic setting of early Tertiary quartzite conglomerates, northwest Wyoming, *in* Koster, E.H., and Steel, R.J., eds., Sedimentology of Gravels and Conglomerates: Canadian Society of Petroleum Geologists, Memoir 10, p. 203–216.

Land Information New Zealand, 1997Christchurch: Topographic map 262-13, 1:250,000 scale, Second Edition.

Lavé, J., and Avouac, J.P., 2001, Fluvial incision and tectonic uplift across the Himalayas of central Nepal: Journal of Geophysical Research, v. 106, p. 26,561–26,591.

Levy, M., and Christie-Blick, N., 1991, Tectonic subsidence of the early Paleozoic passive continental margin in eastern California and southern Nevada: Geological Society of America, Bulletin, v. 103, p. 1590–1606.

Levy, M., Christie-Blick, N., and Link, P.K., 1994, Neoproterozoic incised valleys of the eastern Great Basin, Utah and Idaho: Fluvial response to changes in depositional base level, *in* Dalrymple, R.W., Boyd, R., and Zaitlin, B.A., eds., Incised-Valley Systems: Origin and Sedimentary Sequences: SEPM, Special Publication 51, p. 369–382.

Link, P.K., Christie-Blick, N., Devlin, W.J., Elston, D.P., Horodyski, R.J., Levy, M., Miller, J.M.G., Pearson, R.C., Prave, A., Stewart, J.H., Winston, D., Wright, L.A., and Wrucke, C.T., 1993, Middle and Late Proterozoic stratified rocks of the western U.S. Cordillera, Colorado Plateau, and Basin and Range province, *in* Reed, J.C., Jr., Bickford, M.E., Houston, R.S., Link, P.K., Rankin, D.W., Sims, P.K., and Van Schmus, W.R., eds., Precambrian: Conterminous U.S.: Geological Society of America, The Geology of North America, v. C-2, p. 463–595.

López-Blanco, M., Marzo, M., and Piña, J., 2000, Transgressive–regressive sequence hierarchy of foreland, fan-delta clastic wedges (Montserrat and Sant Llorenç del Munt, middle Eocene, Ebro basin, NE Spain): Sedimentary Geology, v. 138, p. 41–69.

Mardia, K.V., 1972. Statistics of Directional Data: New York, Academic Press, 357 p.

Martins-Neto, M.A., 1996, Lacustrine fan-deltaic sedimentation in a Proterozoic rift basin: the Sopa–Brumadinho Tectonosequence, southeastern Brazil: Sedimentary Geology, v. 106, p. 65–96.

McKee, E.H., 1968, Age and rate of movement of the northern part of the Death Valley–Furnace Creek fault zone, California: Geological Society of America, Bulletin, v. 79, p. 509–512.

McQuarrie, N., and Wernicke, B.P., 2005, An animated tectonic reconstruction of southwestern North America since 36 Ma: Geosphere, v. 1, p. 147–172.

Miall, A.D., 1985, Architectural-element analysis: A new method of facies analysis applied to fluvial deposits: Earth-Science Reviews, v. 22, p. 261–308.

Middleton, G.V., 1965, Antidune cross-bedding in a large flume: Journal of Sedimentary Petrology, v. 35, p. 922–927.

Miller, M.B., and Pavlis, T.L., 2005, The Black Mountains turtlebacks: Rosetta stones of Death Valley tectonics: Earth-Science Reviews, v. 73, p. 115–138.

Miller, M.G., 2003, Basement-involved thrust faulting in a thin-skinned fold-and-thrust belt, Death Valley, California, USA: Geology, v. 31, p. 31–34.

Miller, M.G., and Friedman, R.M., 1999, Early Tertiary magmatism and probable Mesozoic fabrics in the Black Mountains, Death Valley, California: Geology, v. 27, p. 19–22.

Miller, M.G., and Prave, A.R., 2002, Rolling hinge or fixed basin?: A test of continental extensional models in Death Valley, California, United States: Geology, v. 30, p. 847–850.

Nemec, W., Steel, R.J., Porębski, S.J., and Spinnangr, Å., 1984, Domba Conglomerate, Devonian, Norway: Process and lateral variability in a mass flow-dominated, lacustrine fan-delta, *in* Koster, E.H., and Steel, R.J., eds., Sedimentology of Gravels and Conglomerates: Canadian Society of Petroleum Geologists, Memoir 10, p. 295–320.

Niemi, N.A., 2002. Extensional tectonics in the Basin and Range Province and the geology of the Grapevine Mountains, Death Valley region, California and Nevada [Ph.D. thesis]: Pasadena, California Institute of Technology, 337 p.

Niemi, N.A., Wernicke, B.P., Brady, R.J., Saleeby, J.B., and Dunne, G.C., 2001, Distribution and provenance of the middle Miocene Eagle Mountain Formation, and implications for regional kinematic analysis of the Basin and Range province: Geological Society of America, Bulletin, v. 113, p. 419–442.

Noble, L.F., 1941, Structural features of the Virgin Spring area, Death Valley, California: Geological Society of America, Bulletin, v. 52, p. 941–1000.

Prave, A.R., and Wright, L.A., 1986a, Isopach pattern of the Lower Cambrian Zabriskie Quartzite, Death Valley region, California–Nevada: How useful in tectonic reconstructions?: Geology, v. 14, p. 251–254.

Prave, A.R., and Wright, L.A., 1986b, Isopach pattern of the Lower Cambrian Zabriskie Quartzite, Death Valley region, California–Nevada: How useful in tectonic reconstructions? Reply: Geology, v. 14, p. 811–812.

Rice, S., 1998, Which tributaries disrupt downstream fining along gravel-bed rivers?: Geomorphology, v. 22, p. 39–56.

Rust, B.R., 1972, Structure and process in a braided river: Sedimentology, v. 18, p. 221–245.

Rust, B.R., and Koster, E.H., 1984, Coarse alluvial deposits, *in* Walker, R.G., ed., Facies Models: Toronto, Geological Association of Canada, p. 53–67.

Saylor, B.Z., 1991. The Titus Canyon Formation: Evidence for early Oligocene strike slip deformation in the Death Valley area, California, [M.S. thesis]: Cambridge, Massachusetts Institute of Technology, 54 p.

Schlische, R.W., 1991, Half-graben basin filling models: new constraints on continental extensional basin development: Basin Research, v. 3, p. 123–141.

Schlunegger, F., and Schneider, H., 2005, Relief-rejuvenation and topographic length scales in a fluvial drainage basin, Napf area, Central Switzerland: Geomorphology, v. 69, p. 102–117.

Serpa, L., and Pavlis, T.L., 1996, Three-dimensional model of the late Cenozoic history of the Death Valley region, southeastern California: Tectonics, v. 15, p. 1113–1128.

Simons, D.B., and Richardson, E.V., 1966, Resistance to flow in alluvial channels: U.S. Geological Survey, Professional Paper 422-J, 61 p.

Smith, N.D., 1974, Sedimentology and bar formation in the upper Kicking Horse River, a braided outwash stream: Journal of Geology, v. 82, p. 205–223.

Smith, S.A., 1990, The sedimentology and accretionary styles of an ancient gravel-bed stream: the Budleigh Salterton Pebble Beds (Lower Triassic), southwest England: Sedimentary Geology, v. 67, p. 199–219.

Snow, J.K., 1992a, Large-magnitude Permian shortening and continental-margin tectonics in the southern Cordillera: Geological Society of America, Bulletin, v. 104, p. 80–105.

Snow, J.K., 1992b, Paleogeographic and structural significance of an Upper Mississippian facies boundary in southern Nevada and east-central California: Discussion: Geological Society of America, Bulletin, v. 104, p. 1067–1069.

Snow, J.K., and Lux, D.R., 1999, Tectono-sequence stratigraphy of Tertiary rocks in the Cottonwood Mountains and northern Death Valley area, California and Nevada, *in* Wright, L.A., and Troxel, B.W., eds., Cenozoic Basins of the Death Valley Region: Geological Society of America, Special Paper 333, p. 17–64.

Snow, J.K., and Prave, A.R., 1994, Covariance of structural and stratigraphic trends: Evidence for anticlockwise rotation within the Walker Lane belt Death Valley region, California and Nevada: Tectonics, v. 13, p. 712–724.

Snow, J.K., and Wernicke, B., 1989, Uniqueness of geological correlations: An example from the Death Valley extended terrain: Geological Society of America, Bulletin, v. 101, p. 1351–1362.

Snow, J.K., and Wernicke, B., 1993, Large-magnitude Permian shortening and continental-margin tectonics in the southern Cordillera: Reply: Geological Society of America, Bulletin, v. 105, p. 280–283.

Snow, J.K., and Wernicke, B.P., 2000, Cenozoic tectonism in the central Basin and Range: Magnitude, rate, and distribution of upper crustal strain: American Journal of Science, v. 300, p. 659–719.

Snow, J.K., Asmerom, Y., and Lux, D.R., 1991, Permian–Triassic plutonism and tectonics, Death Valley region, California and Nevada: Geology, v. 19, p. 629–632.

Steel, R.J., Mæhle, S., Nilsen, H., Røe, S.L., and Spinnangr, Å., 1977, Coarsening-upward cycles in the alluvium of Hornelen Basin (Devonian) Norway: Sedimentary response to tectonic events: Geological Society of America, Bulletin, v. 88, p. 1124–1134.

Steer, B.L., and Abbott, P.L., 1984, Paleohydrology of the Eocene Ballena gravels, San Diego County, California: Sedimentary Geology, v. 38, p. 181–216.

Stevens, C.H., and Stone, P., 1988, Early Permian thrust faults in east-central California: Geological Society of America, Bulletin, v. 100, p. 552–562.

Stevens, C.H., and Stone, P., 2005, Interpretation of the Last Chance thrust, Death Valley region, California, as an Early Permian décollement in a previously undeformed shale basin: Earth-Science Reviews, v. 73, p. 79–101.

Stevens, C.H., Stone, P., and Belasky, P., 1991, Paleogeographic and structural significance of an Upper Mississippian facies boundary in southern Nevada and east-central California: Geological Society of America, Bulletin, v. 103, p. 876–885.

Stevens, C.H., Stone, P., and Belasky, P., 1992, Paleogeographic and structural significance of an Upper Mississippian facies boundary in southern Nevada and east-central California: Reply: Geological Society of America, Bulletin, v. 104, p. 1069–1071.

Stewart, J.H., 1967, Possible large right-lateral displacement along fault and shear zones in the Death Valley–Las Vegas area, California and Nevada: Geological Society of America, Bulletin, v. 78, p. 131–142.

Stewart, J.H., 1972, Initial deposits in the Cordilleran geosyncline: Evidence of a Late Precambrian (< 850 m.y.) continental separation: Geological Society of America, Bulletin, v. 83, p. 1345–1360.

Stewart, J.H., 1983, Extensional tectonics in the Death Valley area, California: Transport of the Panamint Range structural block 80 km northwestward: Geology, v. 11, p. 153–157.

Stewart, J.H., 1986, Isopach pattern of the Lower Cambrian Zabriskie Quartzite, Death Valley region, California–Nevada: How useful in tectonic reconstructions? Comment: Geology, v. 14, p. 810–811.

Stewart, J.H., Albers, J.P., and Poole, F.G., 1968, Summary of regional evidence for right-lateral displacement in the western Great Basin: Geological Society of America, Bulletin, v. 79, p. 1407–1414.

Stewart, J.H., Albers, J.P., and Poole, F.G., 1970, Summary of regional evidence for right-lateral displacement in the western Great Basin: Reply: Geological Society of America, Bulletin, v. 81, p. 2175–2180.

Stone, P., and Stevens, C.H., 1993, Large-magnitude Permian shortening and continental-margin tectonics in the southern Cordillera: Discussion: Geological Society of America, Bulletin, v. 105, p. 279–280.

Streitz, R., and Stinson, M.C., 1974, Geologic Map of California: Death Valley Sheet: Sacramento, California Department of Conservation, Division of Mines and Geology.

Topping, D.J., 1993, Paleogeographic reconstruction of the Death Valley extended region: Evidence from Miocene large rock-avalanche deposits in the Amargosa Chaos basin, California: Geological Society of America, Bulletin, v. 105, p. 1190–1213.

Troxel, B.W., 1989, Shoshone to eastern Funeral Range, *in* Cooper, J.D., ed., Cavalcade of Carbonates: SEPM, Pacific Section, Field Trip 3, Volume and Guidebook, p. 32–36.

Troxel, B.W., and Heydari, E., 1982, Basin and Range geology in a roadcut, *in* Cooper, J.D., Troxel, B.W., and Wright, L.A., eds., Geology of Selected Areas in the San Bernardino Mountains, Western Mojave Desert, and Southern Great Basin, California: Geological Society of America, Cordilleran Section, v. 9, p. 91–96.

Tucker, M.E., 1996. Sedimentary Rocks in the Field: New York, John Wiley & Sons, 153 p.

Wernicke, B., 1992, Cenozoic extensional tectonics of the U.S. Cordillera, *in* Burchfiel, B.C., Lipman, P.W., and Zoback, M.L., eds., The Cordilleran Orogen: Conterminous U.S.: Geological Society of America, The Geology of North America, v. G-3, p. 553–581.

Wernicke, B., 1993, A new measurement of Cenozoic crustal extension across the central Death Valley region, Basin and Range Province (abstract): Geological Society of America, Annual Meeting, Abstracts with Programs, v. 25, p. A-352.

Wernicke, B., Axen, G.J., and Snow, J.K., 1988a, Basin and Range extensional tectonics at the latitude of Las Vegas, Nevada: Geological Society of America, Bulletin, v. 100, p. 1738–1757.

Wernicke, B., Snow, J.K., and Walker, J.D., 1988b, Correlation of early Mesozoic thrusts in the southern Great Basin and their possible indication of 250–300 km of Neogene crustal extension, *in* Weide, D.L., and Faber, M.L., eds., This Extended Land: Geological Journeys in the Southern Basin and Range: Geological Society of America, Cordilleran Section Meeting, Field Trip Guidebook, p. 255–267.

Wernicke, B.P., Walker, J.D., and Hodges, K.V., 1988c, Field guide to the northern part of the Tucki Mountain fault system, Death Valley region, California, *in* Weide, D.L., and Faber, M.L., eds., This Extended Land: Geological Journeys in the Southern Basin and Range: Geological Society of America, Cordilleran Section Meeting, Field Trip Guidebook, p. 58–63.

Wernicke, B.P., Axen, G.J., and Snow, J.K., 1990, Basin and Range extensional tectonics at the latitude of Las Vegas, Nevada: Reply: Geological Society of America, Bulletin, v. 102, p. 269–270.

Willis, B., 1993, Evolution of Miocene fluvial systems in the Himalayan foredeep through a two kilometer-thick succession in northern Pakistan: Sedimentary Geology, v. 88, p. 77–121.

Wright, L.A., and Prave, A.R., 1993, Proterozoic–Early Cambrian Tectonostratigraphic record in the Death Valley region, California–Nevada, *in* Reed, J.C., Jr., Bickford, M.E., Houston, R.S., Link, P.K., Rankin, D.W., Sims, P.K., and Van Schmus, W.R., eds., Precambrian: Conterminous U.S.: Geological Society of America, The Geology of North America, v. C-2, p. 529–533.

Wright, L.A., and Troxel, B.W., 1967, Limitations on right-lateral, strike-slip displacement, Death Valley and Furnace Creek fault zones, California: Geological Society of America, Bulletin, v. 78, p. 933–950.

Wright, L.A., and Troxel, B.W., 1970, Summary of regional evidence for right-lateral displacement in the western Great Basin: Discussion: Geological Society of America, Bulletin, v. 81, p. 2167–2173.

Wright, L.A., and Troxel, B.W., 1973, Shallow-fault interpretation of Basin and Range structure, southwestern Great Basin, *in* DeJong, K.A., and Scholten, R., eds., Gravity and Tectonics: New York, John Wiley & Sons, p. 397–407.

Wright, L.A., and Troxel, B.W., 1984. Geology of the north 1/2 Confidence Hills 15′ Quadrangle, Inyo County, California: Sacramento, California Department of Conservation, Division of Mines and Geology, Map Sheet 34.

Wright, L.A., Troxel, B.W., Burchfiel, B.C., Chapman, R.H., and Labotka, T.C., 1981, Geologic cross section from the Sierra Nevada to the Las Vegas Valley, eastern California to southern Nevada: Geological Society of America, Map and Chart Series, MC-28M.

Wright, L.A., Thompson, R.A., Troxel, B.W., Pavlis, T.L., Dewitt, E.H., Otton, J.K., Ellis, M.A., Miller, M.G., and Serpa, L.F., 1991, Cenozoic magmatic and tectonic evolution of the east-central Death Valley region, California, *in* Walawender, M.J., and Hanan, B.B., eds., Geological Excursions in Southern California and Mexico: Geological Society of America, Annual Meeting, Guidebook, p. 93–127.

Wright, L.A., Greene, R.C., Çemen, I., Johnson, F.C., and Prave, A.R., 1999, Tectonostratigraphic development of the Miocene–Pliocene Furnace Creek Basin and related features, Death Valley region, California, *in* Wright, L.A., and Troxel, B.W., eds., Cenozoic Basins of the Death Valley Region: Geological Society of America, Special Paper 333, p. 87–114.

Received 23 February 2007; accepted 16 September 2007.